Electronic Journal of Applied Statistical Analysis
EJASA, Electron. J. App. Stat. Anal.
http://siba-ese.unisalento.it/index.php/ejasa/index
e-ISSN: 2070-5948
DOI: 10.1285/i20705948v16n3p654

Classical and Bayesian Estimations for a 2-Component Generalized Rayleigh Mixture Model under Type I Censoring

By Dey et al.

15 December 2023

Electronic Journal of Applied Statistical Analysis
Vol. 16, Issue 3, 2023, 654-693
DOI: 10.1285/i20705948v16n3p654

Classical and Bayesian Estimations for a 2-Component Generalized Rayleigh Mixture Model under Type I Censoring

Sanku Dey[a], Mohammed K. Shakhatreh*[b], Kundan Singh[c], Amulya Kumar Mahto[d], and Yogesh Mani Tripathi[c]

[a]*Department of Statistics, St. Anthony's College, Shillong, Meghalaya, India*
[b]*Department of Mathematics and Statistics, Jordan University of Science and Technology, Jordan*
[c]*Department of Mathematics, Indian Institute of Technology, Patna, Bihar, India*
[d]*Mehta Family School of Data Science and Artificial Intelligence, Indian Institute of Technology, Guwahati, Assam, India*

15 December 2023

Mixture models are more appealing and appropriate for studying the heterogeneous nature of lifetimes of certain mechanical, biological, social, economic and several other processes as compared to simple models. This paper considers a mixture of generalized Rayleigh distributions under classical and Bayesian perspectives based on type I censored samples. The new distribution which exhibits decreasing, decreasing-increasing-decreasing, unimodal and bimodal shaped density while the distribution has the ability to model lifetime data with increasing, increasing-decreasing-increasing, bathtub and bi-bathtub-shaped failure rates. We derive some basic and structural properties of the proposed distribution. Moreover, we estimate the parameters of the model by using frequentist and Bayesian approaches. In frequentist method, the maximum likelihood estimate of the parameters and their asymptotic confidence intervals are obtained while for Bayesian analysis, the squared error loss (SEL) function and uniform as well as beta and gamma priors are considered to obtain the Bayes estimators of the unknown parameters of the model. Furthermore, the highest posterior density (HPD) credible intervals are also obtained. In real data analysis, in addition to point estimates of the model parameters, asymptotic confidence intervals and HPD credible

*Corresponding author: mkshakhatreh6@just.edu.jo.

ISSN: 2070-5948
http://siba-ese.unisalento.it/index.php/ejasa/index

intervals, two bootstrap CIs are also provided. Monte Carlo simulation study is performed to assess the behavior of these estimators. An application of the model is presented by re-analyzing strength for single carbon fibers data set.

Keywords: Bayesian analysis, censored data, generalized Rayleigh distribution, mixture model, squared error loss function.

1 Introduction

In general, the study of homogeneous data is wide, where data is mostly considered as having a single population with a single pattern of failure. But in real life, we often come across heterogeneous data comprising of multiple sub-populations coming from different environments. For example, a life time experiment data may have multiple sub-populations which may be due to different manufacturing processes or different experimental environments of the units. Therefore, the methodological development and practical applications of finite mixtures of lifetime distributions have stimulated great interest in recent times. This can mainly be attributed to the versatility of the mixture models and their potential applicability in real life situations. For example, Mendenhall and Hader (1958) have opined that there are mainly two or more different causes attributable to the failure of a system or device in practical situations encountered by engineers. Similarly, in order to know the proportion of failure due to a certain cause, Acheson and McElwee (1953) divided the causes of failures of electronic tubes into gaseous defects, mechanical defects and normal deterioration of the cathode. Another example is that of an engineering system which consists of different subsystems. These subsystems may be composed of different homogeneous and/or heterogeneous subsystems and in such cases, single probability models fail to capture the heterogeneous nature of the systems. Therefore, researchers use a mixture model to capture the heterogeneity of such systems. Finite mixture models of some suitable probability distribution have been garnering popular attention primarily because of the fact that most of the time, the commonly used distributions seem to be redundant when a population comprising several subpopulations mixed in unknown proportions is considered. Mixture models are directly applicable when data are available only from overall mixture distributions, such as data arising from the field of biology; Bhattacharya (1967); Gregor (1969), medicine; Chivers (1977); Burckhardt (1978)), social sciences; Harris (1983), economics; Jedidi et al. (1997) and Shakhatreh et al. (2019), reliability analysis; Sultan et al. (2007), life testing; Shawky and Bakoban (2009), industrial engineering; Ali et al. (2012), etc. Based on different components of the mixture model coming from same or different family of distributions, the mixture models are categorized as type-I and type-II mixture models. If components of the probability distribution of the mixture model belong to the same family, it is classified as type-I mixture model, and if the components come from different families, it is classified as type-II mixture model. The features of these models have been studied in detail by Li and Sedransk (1988).

Lately, researchers have taken a keen interest in studying mixture models from classical and Bayesian perspectives, particularly mixture models with finite and infinite components. It was Newcomb (1886) who first developed the concept of the finite mixture distribution for modelling outliers. Since then several studies have been conducted on classical and Bayesian analysis of a two-component mixture model. Notable among them are: Sankaran and Nair (2005) , Nadarajah and Kotz (2005), Sultan et al. (2007), Kalantan and F. (1988), Aslam1 et al. (2015), Alotaibi et al. (2022), Li and Fang (2022), Al-Hemyari and Al Abbasi (2023) and many others. One may also refer some of the recent articles with respect to censoring schemes based on classical and Bayesian estimation of parameters of mixture models. For example, Saleem et al. (2010), Feroze and Aslam (2014), Ali (2014), Tahir et al. (2016, 2019), Sindhu et al. (2018), Aslam et al. (2018, 2020), Feroze et al. (2021), Bdair and Raqab (2022), Jahanbani et al. (2023) and references cited therein.

Generalized Rayleigh distribution, also widely known as Burr X distribution, is well discussed with its applicability and relation with other well-known distributions. This distribution has many properties common to many distributions like two parameter gamma, Weibull and generalized exponential distributions. The additional property of the non-monotone hazard rate makes this distribution very useful in modelling many real-life problems. Thus, a mixture of generalized Rayleigh components becomes more flexible and useful in modelling many real-life problems where data are heterogeneously distributed. Motivated by this rationale, our goal of this paper is to introduce a 2-component mixture of generalized Rayleigh distribution called the mixture of two component generalized Rayleigh (MTGR) distribution. Several properties of the new distribution including the identifiability of the distribution are derived. Next, we estimate the parameters of the model by using frequentist and Bayesian approaches using type I censored samples. In frequentist case, the maximum likelihood method is used to estimate the model parameters. Also, approximate confidence intervals (ACIs) of the model parameters are obtained. For Bayesian analysis, squared error loss function and uniform, as well as beta and gamma priors, are considered to obtain the Bayes estimators. Besides, the highest posterior density (HPD) credible intervals are also obtained. In real data analysis, over and above point estimates, ACIs and HPD credible intervals, we have also considered two bootstrap CIs. To the best of our knowledge, 2-component mixture of generalized Rayleigh distributions is not discussed before using the aforementioned methods of estimation.

The article is organized as follows. In Section 2, we introduce the 2-component mixture of generalized Rayleigh distributions. Shape properties of the PDF and HRF of the 2-component mixture of generalized Rayleigh distributions are presented in Section 3. In Section 4, some statistical properties of MTGR distribution are presented. The identifiability of MTGR distribution are shown in Section 5. In Section 6, the estimation of the model parameters under type I censored samples are obtained and discussed by the methods of maximum likelihood, bootstrap confidence intervals (CIs), and Bayes methods using the Metropolis-Hastings (MH) algorithm. The Monte Carlo simulation study is carried out in Section 7. In Section 8, the potentiality of the new model is illustrated by real data. Finally, some concluding remarks and further research proposals are given in Section 9.

2 Two-component mixture of generalized Rayleigh (GR) distribution

In this section, we introduce the finite mixtures of two-component of GR distribution, see, Surles and Padgett (2001). Several authors considered different aspects of GR distribution. See for example, Kundu and Raqab (2005), Yakubu and Yahaya (2015), Dey et al. (2017), Junru and Wenhao (2020), Mahto et al. (2018) and many others. First, we recall the definition of the GR distribution and some of its properties. A random variable X is called a GR random variable with shape and inverted scale parameters; $\alpha > 0$ and $\lambda > 0$, respectively, if its PDF is given by

$$f(x;\alpha,\lambda) = 2\alpha\lambda^2\ x\ \exp[-(\lambda x)^2]\left(1-\exp[-(\lambda x)^2]\right)^{\alpha-1}; \qquad x>0, \tag{1}$$

and the corresponding cumulative distribution function (CDF)can be expressed as

$$F(x;\alpha,\lambda) = \left(1-\ \exp[-(\lambda x)^2]\right)^{\alpha}; \qquad x>0\,, \alpha,\lambda>0 \tag{2}$$

The reliability function (RE) is given by

$$R(x;\alpha,\lambda) = 1-\left(1-\ \exp[-(\lambda x)^2]\right)^{\alpha} \tag{3}$$

and the hazard rate (HR) function is given by

$$H(x;\alpha,\lambda) = \frac{2x\alpha\lambda^2\ \exp[-(\lambda x)^2]}{1-(1-\ \exp[-(\lambda x)^2])^{\alpha}}. \tag{4}$$

Note that the generalized Rayleigh is a special case of the exponentiated Weibull distribution introduced and discussed by Mudholkar et al. (1995) with CDF; $F(x) = (1-\exp(-(\lambda\, x)^c)^{\alpha}$. They showed that the hazard rate function of exponentiated Weibull distribution can be constant ($\alpha = c = 1$), decreasing ($c < 1$ and $c\alpha < 1$), increasing ($c > 1$ and $c\alpha > 1$), or unimodal ($c < 1$ and $c\alpha > 1$) and bathtub-shaped failure rates (($c > 1$ and $c\alpha < 1$). Therefore, the shapes of the HR function of the GR distribution can be monotonically increasing or bathtub-shaped hazard rates.

The finite mixture of two components of GR distribution assuming unknown mixing weights (proportions) p_1 and p_2 is defined via its PDF as follows:

$$f(x;\boldsymbol{\zeta}) = p_1 f_1(x;\boldsymbol{\theta}_1) + p_2 f_2(x;\boldsymbol{\theta}_2); \qquad p_1+p_2=1, \tag{5}$$

where $\boldsymbol{\zeta} = (p_i,\boldsymbol{\theta}_i)$, $\boldsymbol{\theta}_i = (\alpha_i,\lambda_i),\ i=1,2,$ and $f_i(x;\boldsymbol{\theta}_i)$ is the pdf of the i^{th} component given via Eq.(1) with parameters α_i and λ_i. Equivalently,

$$f(x) = \sum_{i=1}^{2} p_i \left\{2\alpha_i\lambda_i^2 x\exp[-(\lambda_i x)^2]\left(1-\exp[-(\lambda_i x)^2]\right)^{(\alpha_i-1)}\right\} \tag{6}$$

Henceforth, we use $X \sim \text{MTGR}(p, \alpha_1, \alpha_2, \lambda_1, \lambda_2)$ to stand for a random variable whose PDF is given via Eq.(6).

The MTGR distribution can be in principle useful in studying the failure of a certain device that is primarily damaged due to two failure types with unequal effects, one of which follows the GR(α_1, λ_1) distribution and which occurs with probability p_1 whereas the other type follows another GR(α_2, λ_2) distribution but with probability $1-p_1$, being either of these type failures can lead to the device's failure An interesting example that describes this situation, suppose that punctures and cumulative damage are identified as the two main types of failure for a certain car tire. Clearly, the tire will break down once one of these types of failures has arisen. Observe that the dominant cause of failures is ageing, however, random failures due to puncture can remain. So if failure due to the dominant ones (ageing) follows the GR(α_1, λ_1)distribution that occurred with probability p_1 whereas the failure due to punctures follows another GR(α_2, λ_2) distribution with probability $1-p_1$, then the failure of the tire can be studied using the distribution given via Eq.(6).

The CDF, RE, and HR functions of the MTGR distribution are given respectively in the following compact forms

$$F(x) = p\left(1-\exp[-(\lambda_1 x)^2]\right)^{\alpha_1} + (1-p)\left(1-\exp[-(\lambda_2 x)^2]\right)^{\alpha_2}, \tag{7}$$

$$R(x) = 1 - p\left(1-\exp[-(\lambda_1 x)^2]\right)^{\alpha_1} - (1-p)\left(1-\exp[-(\lambda_2 x)^2]\right)^{\alpha_2}, \tag{8}$$

and

$$H(x) = \frac{\sum_{i=1}^{2} p_i \left\{2\alpha_i \lambda_i^2 x \exp[-(\lambda_i x)^2]\left(1-\exp[-(\lambda_i x)^2]\right)^{(\alpha_i-1)}\right\}}{1-p\left(1-\exp[-(\lambda_1 x)^2]\right)^{\alpha_1} - (1-p)\left(1-\exp[-(\lambda_2 x)^2]\right)^{\alpha_2}}, \tag{9}$$

where $p = p_1$.

3 Properties of PDF and HR curves

In this section, we study and demonstrate the possible shapes for the PDF and HR curves of the MTGR distribution.

3.1 Shapes of the PDF

Before we start discussing shapes for the PDF curves of the MTGR distribution, we have the following proposition

Proposition 1. *We have that*

1. *For sufficiently small values of* x, ($x \to 0$) *and for* $i \neq j$, $i, j = 1, 2$, *we have that*

$$\lim_{x\to 0} f(x, \boldsymbol{\zeta}) = \begin{cases} \infty, & \alpha_i < \alpha_i \leq \frac{1}{2} \text{ or } (\alpha_i < \frac{1}{2} \text{ and } \alpha_j \geq \frac{1}{2}), \\ \\ 0, & \alpha_i, \alpha_j \geq \frac{1}{2}, \end{cases}$$

2. For sufficiently, large values of x, ($x \to \infty$,) we have that $\lim_{x\to\infty} f(x,\boldsymbol{\zeta}) = 0$.

Proof. For (1), observe that as $x \to 0$, we have $1 - \exp[-(\lambda_i x)^2] \sim \lambda_i^2 x^2, \quad i = 1, 2.$ Consequently, we have

$$f(x,\boldsymbol{\zeta}) \sim 2\alpha_1 \lambda_1^{2\alpha_1} p \; x^{2\alpha_1 - 1} + 2\alpha_2 \lambda_2^{2\alpha_2}(1-p) \; x^{2\alpha_2 - 1}. \tag{10}$$

When both α_1 and α_2 are greater than or equal to 1/2, it then follows from Eq.(10) that $f(x,\boldsymbol{\zeta}) \to 0$ as $x \to 0$. Next, re-writing Eq.(10) as follows: if $\alpha_1 < \alpha_2 \le \frac{1}{2}$ or ($\alpha_1 < \frac{1}{2}$ and $\alpha_2 \ge \frac{1}{2}$), then

$$f(x,\boldsymbol{\zeta}) = 2x^{2\alpha_1 - 1}\left[\alpha_1 \lambda_1^{2\alpha_1} p + \alpha_2 \lambda_2^{2\alpha_2}(1-p) x^{2(\alpha_2 - \alpha_1)}\right],$$

and when $\alpha_2 < \alpha_1 \le \frac{1}{2}$ or ($\alpha_1 \ge \frac{1}{2}$ and $\alpha_2 < \frac{1}{2}$), then

$$f(x,\boldsymbol{\zeta}) = 2x^{2\alpha_2 - 1}\left[\alpha_1 \lambda_1^{2\alpha_1} p x^{2(\alpha_1 - \alpha_2)} + \alpha_2 \lambda_2^{2\alpha_2}(1-p)\right].$$

Therefore, $f(x,\boldsymbol{\zeta}) \to \infty$ as $x \to 0$. For (2), as $x \to \infty$, we have

$$f(x) \sim p \; 2\alpha_1 \lambda_1^2 \; x \exp[-(\lambda_1 x)^2] + (1-p) \; 2\alpha_2 \lambda_2^2 x \; \exp[-(\lambda_2 x)^2].$$

On using the above equation along with the aid of the L'Hoptials rule, we conclude that $f(x) \to 0$ as $x \to \infty$. □

The behaviour of the PDF of the MTGR model can be summarized in four cases.

- Decreasing case. This case occur when $\alpha_1, \alpha_2 < 1/2$. To show this, we have from 1 that $f(x,\boldsymbol{\zeta}) \to \infty$, as $x \to 0$ and $f(x,\boldsymbol{\zeta}) \to, 0$ as $x \to \infty$. To finish, we need to show that the first derivative of $f(x,\boldsymbol{\zeta})$ is negative. The first derivative of Eq.(6) is

  $$f^{'}(x;\boldsymbol{\zeta}) = \sum_{i=1}^{2} p_i \; g_i(x,\boldsymbol{\theta}_i) w_i(x,\boldsymbol{\theta}_i), \quad p_1 + p_2 = 1, \tag{11}$$

  where $g_i(x,\boldsymbol{\theta}_i) = 2\lambda_i^2 \alpha_i \; \exp[-(\lambda_i x)^2]\left(1 - \exp[-(\lambda_i x)^2]\right)^{(\alpha_i - 2)}$ and

  $$w_i(x,\boldsymbol{\theta}_i) = \left[1 - 2\lambda_i^2 x^2 - \exp[-(\lambda_i x)^2]\left(1 - 2\alpha_i \lambda_i^2 x^2\right)\right].$$

  If $\alpha_i < 1/2$, then $\left(1 - 2\alpha_i \lambda_i^2 x^2\right) > \left(1 - \lambda_i^2 x^2\right)$, and hence, it can be checked that $w_i(x,\boldsymbol{\theta}_i) < 0$. Since $g_i(x,\boldsymbol{\theta}_i) > 0$ and $w_i(x,\boldsymbol{\theta}_i) < 0$, it then follows that the first derivative of the PDF for the i^{th} component is negative, i.e., $f_i^{'}(x;\boldsymbol{\theta}_i) < 0$, and so is $f^{'}(x;\boldsymbol{\zeta}) < 0$. See Figures 1

- Decreasing-increasing-decreasing case. This case happens when $\alpha_i < \frac{1}{2}$ and $\alpha_j \ge \frac{1}{2}$, $i \ne j, \; i,j = 1,2$. To see this, assume without loss of generality that $\alpha_1 < 1/2$ and that $\alpha_2 > 1/2$. In this case $f_1(x;\boldsymbol{\theta}_1)$ is a decreasing function whereas $f_2(x;\boldsymbol{\theta}_2)$ is a unimodal function. Clearly, the decreasing-increasing-decreasing case can occur due to the intersection of the two functions, which is quite natural. See Figure 2 (a- c).

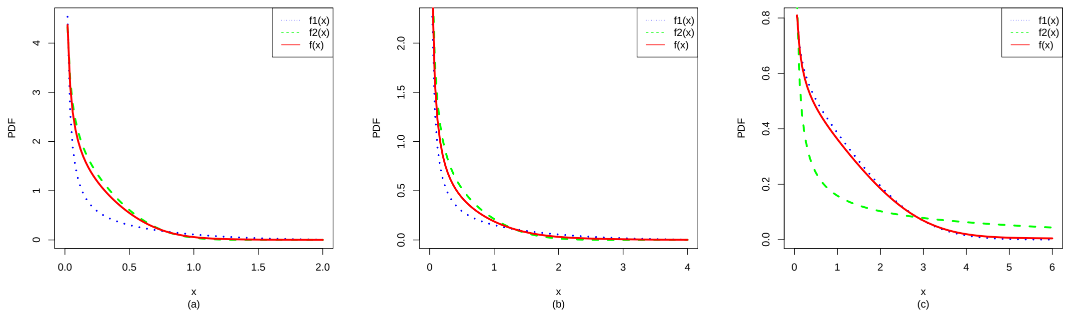

Figure 1: plots of the MTGR distribution exhibiting decreasing function for the cases: (a) ($p = 0.2$, $\alpha_1 = 0.1$, $\alpha_2 = 0.3$, $\lambda_1 = 1$, $\lambda_2 = 2$); (b) ($p = 0.4$, $\alpha_1 = 0.1$, $\alpha_2 = 0.2$, $\lambda_1 = 0.5$, $\lambda_2 = 2$); (c) ($p = 0.9$, $\alpha_1 = 0.4$, $\alpha_2 = 0.2$, $\lambda_1 = 0.5$, $\lambda_2 = 0.1$)

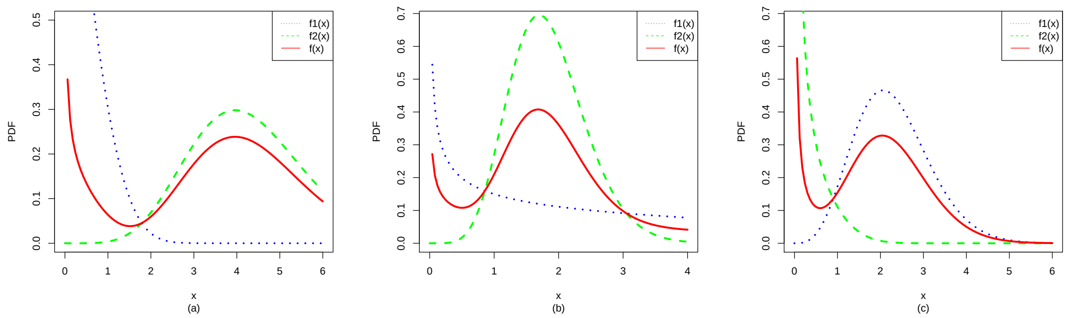

Figure 2: plots of the MTGR distribution exhibiting decreasing function for the cases: (a)($p = 0.2$, $\alpha_1 = 0.1$, $\alpha_2 = 0.3$, $\lambda_1 = 3$, $\lambda_2 = 0.3$); (b)($p = 0.5$, $\alpha_1 = 0.3$, $\alpha_2 = 3$, $\lambda_1 = 0.1$, $\lambda_2 = 0.7$); (c) ($p = 0.7$, $\alpha_1 = 2$, $\alpha_2 = 0.1$, $\lambda_1 = 0.5$, $\lambda_2 = 1$)

- Unimodal case. This case can happen when $\alpha_1,\ \alpha_2 > 1/2$. Note that when $\alpha_i > 1/2$, then $f_i(x;\boldsymbol{\theta}_i)$ has a unique mode. Let $x_i^\star$ be the mode of $f_i(x;\boldsymbol{\theta}_i)$, for $i = 1, 2$. Put $x_1 = \min(x_1^\star, x_2^\star)$ and $x_2 = \max(x_1^\star, x_2^\star)$. Since the PDF of the MTGR distribution is a mixture of $f_1(x;\boldsymbol{\theta}_1)$ and $f_2(x;\boldsymbol{\theta}_2)$, then certainly $f(x;\boldsymbol{\zeta})$ will possess a unique mode when the modes $x_1^\star$ and $x_2^\star$ are relatively close. It is observed that these two modes can be close from each other when $\alpha_1 < \alpha_2$ and $\lambda_1 < \lambda_2$ or vice versa, see for example Figure 3(a-c).

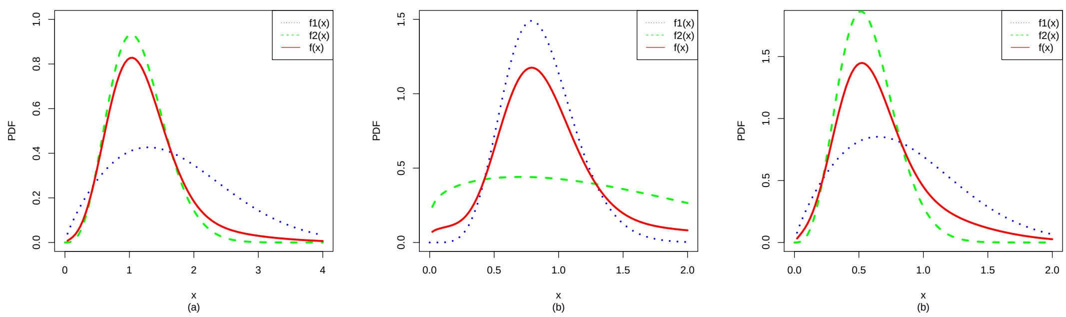

Figure 3: plots of the MTGR distribution exhibiting exhibiting unimodal: (a) ($p = 0.2$, $\alpha_1 = 0.9$, $\alpha_2 = 2$, $\lambda_1 = 0.5$, $\lambda_2 = 1$); (b) ($p = 0.7$, $\alpha_1 = 3$, $\alpha_2 = 0.6$, $\lambda_1 = 1.5$, $\lambda_2 = 0.5$); (c) ($p = 0.4$, $\alpha_1 = 0.9$, $\alpha_2 = 2$, $\lambda_1 = 1$, $\lambda_2 = 2$)

- Bimodal case. The bimodal case can occur when modes $x_1^\star$ and $x_2^\star$ (defined in the previous case) are far from each other. It is anticipated that this case can happen when either $\alpha_1 > \alpha_2$ and $\lambda_1 < \lambda_2$ or $\alpha_1 < \alpha_2$ and $\lambda_1 > \lambda_2$. See Figure 4(a-c) for further illustration.

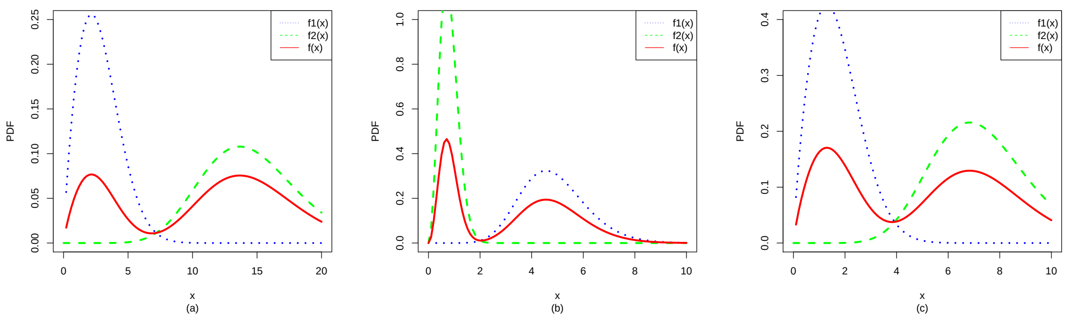

Figure 4: plots of the MTGR distribution exhibiting bimodals for the cases: (a) ($p = 0.3$, $\alpha_1 = 0.9$, $\alpha_2 = 5$, $\lambda_1 = 0.3$, $\lambda_2 = 0.1$); (b) ($p = 0.6$, $\alpha_1 = 5$, $\alpha_2 = 1.5$, $\lambda_1 = 0.3$, $\lambda_2 = 1.3$); (c) ($p = 0.4$, $\alpha_1 = 0.9$, $\alpha_2 = 5$, $\lambda_1 = 0.5$, $\lambda_2 = 0.2$)

3.2 Shapes of the HR curves

Al-Hussaini and Sultan (2001) provided a general result about the hazard rate function for any mixture of two distribution functions in terms of corresponding hazard rate functions to these distributions. Therefore, the hazard rate function in Eq.(4) can be penned in view of this result as a convex combination of two GR hazard rate functions. That is, the HR can be written as follows

$$H(x;\boldsymbol{\zeta}) = g(x;\boldsymbol{\zeta})H_1(x;\boldsymbol{\theta}_1) + (1-g(x;\boldsymbol{\zeta}))H_2(x;\boldsymbol{\theta}_2), \tag{12}$$

where for $i=1,2$, $H_i(x;\boldsymbol{\theta}_i)$ is the HR function of the GR given in Eq. (4) and

$$g(x;\boldsymbol{\zeta}) = \frac{1}{1+k(x;\boldsymbol{\zeta})} \quad \text{and} \quad k(x;\boldsymbol{\zeta}) = \frac{(1-p)R_2(x;\boldsymbol{\theta}_2)}{pR_1(x;\boldsymbol{\theta}_1)}.$$

The first derivative of the HR function of the MTGR distribution based on Eq.(12) is given by

$$\begin{aligned} H^{'}(x;\boldsymbol{\zeta}) &= g(x;\boldsymbol{\zeta})H_1^{'}(x;\boldsymbol{\theta}_1) + q(x;\boldsymbol{\zeta}))H_2^{'}(x;\boldsymbol{\theta}_2) \\ &\quad - g(x;\boldsymbol{\zeta})q(x;\boldsymbol{\zeta})\left[H_1(x;\boldsymbol{\theta}_1) - H_2(x;\boldsymbol{\theta}_2)\right]^2, \end{aligned} \tag{13}$$

where $q(x;\boldsymbol{\zeta}) = 1-g(x;\boldsymbol{\zeta})$. The following proposition is helpful in describing the possible shapes for the HR curves.

Proposition 2. *For the HR function given via Eq.*(12)*, we have that*

1. *For sufficiently small values of x, $(x \to 0)$ and for $i \neq j,\ i,j = 1,2$*

$$\lim_{x\to 0} H(x,\boldsymbol{\zeta}) = \begin{cases} \infty, & \alpha_i < \alpha_i \leq \frac{1}{2} \ \ or \ \ (\alpha_i < \frac{1}{2} \ and \ \alpha_j \geq \frac{1}{2}), \\ \\ 0, & \alpha_i, \alpha_j \geq \frac{1}{2} \end{cases}$$

2. *For sufficiently, large values of x,$(x \to \infty,)$ we have that* $\lim_{x\to\infty} H(x,\boldsymbol{\zeta}) = \infty$.

Proof. For (1), it follows from Proposition 1 by noting that $\lim_{x\to 0} f(x) = \lim_{x\to 0} H(x)$. To show (2), first not that $\lim_{x\to\infty} H_i(x;\boldsymbol{\theta}_i) = \infty$, for $i=1,2$. This can be verified by using L'Hoptial's rule. Now consider the behavior of $k(x,\boldsymbol{\zeta})$ as $x\to\infty$. Since

$$\begin{aligned} \lim_{x\to\infty} k(x;\boldsymbol{\zeta}) &= \frac{(1-p)}{p} \lim_{x\to\infty} \frac{1-\left(1-\ \exp[-(\lambda_2 x)^2]\right)^{\alpha_2}}{1-(1-\ \exp[-(\lambda_1 x)^2])^{\alpha_1}} \\ &\doteq \frac{(1-p)}{p}\left(\frac{\alpha_2\lambda_2^2}{\alpha_1\lambda_1^2}\right) \lim_{x\to\infty} D(F_1,F_2;x) \lim_{x\to\infty} \boldsymbol{\Lambda}(\lambda_1,\lambda_2;x) \exp\left[-(\lambda_2^2-\lambda_1^2)x^2\right], \end{aligned}$$

where $\doteq$ denotes that L'Hoptial's rule is used,

$$D(F_1,F_2;x) = \frac{\left(1-\ \exp[-(\lambda_2 x)^2]\right)^{\alpha_2-1}}{(1-\ \exp[-(\lambda_1 x)^2])^{\alpha_1-1}} \quad \text{and} \quad \boldsymbol{\Lambda}(\lambda_1,\lambda_2;x) = \exp\left[-(\lambda_2^2-\lambda_1^2)x^2\right].$$

Clearly, $D(F_1, F_2; x) \to 1$ as $x \to \infty$. Since,

$$\lim_{x\to\infty} \mathbf{\Lambda}(\lambda_1, \lambda_2; x) = \begin{cases} \infty, & \lambda_1^2 > \lambda_2^2 \\ 1, & \lambda_1^2 = \lambda_2^2, \\ 0, & \lambda_1^2 < \lambda_2^2 \end{cases}$$

it then follows that

$$\lim_{x\to\infty} k(x; \boldsymbol{\zeta}) = \begin{cases} \infty, & \lambda_1^2 > \lambda_2^2 \\ \frac{(1-p)}{p}, & \lambda_1^2 = \lambda_2^2 \\ 0, & \lambda_1^2 < \lambda_2^2 \end{cases}$$

Now for $\lambda_1^2 > \lambda_2^2$ and as $x \to \infty$, we have that $g(x; \boldsymbol{\zeta}) \to 0$, and hence $H(x; \boldsymbol{\zeta}) \sim H_2(x, \boldsymbol{\theta}_2)$. Consequently, we have that $\lim_{x\to\infty} H(x; \boldsymbol{\zeta}) = \lim_{x\to\infty} H_2(x, \boldsymbol{\theta}_2) = \infty$. Similarly, when $\lambda_1^2 < \lambda_2^2$ then $g(x; \boldsymbol{\zeta}) \to 1$ as $x \to \infty$, and so $H(x; \boldsymbol{\zeta}) \sim H_1(x, \boldsymbol{\theta}_1)$. An immediate result is that $\lim_{x\to\infty} H(x; \boldsymbol{\zeta}) = \lim_{x\to\infty} H_1(x, \boldsymbol{\theta}_1) = \infty$. When $\lambda_1^2 = \lambda_2^2$, write Eq.(4) as follows

$$HR(x; \boldsymbol{\zeta}) = pH_1(x, \boldsymbol{\theta}_1) \left[1 + \frac{(1-p)}{p})D(H_1, H_2; x)\right],$$

where $D(H_1, H_2; x) = H_2(x, \boldsymbol{\theta}_2)/H_2(x, \boldsymbol{\theta}_1)$. As $x \to \infty$ we have that $D(H_1, H_2; x) \to 1$. Therefore, we have that $HR(x; \boldsymbol{\zeta}) \sim H_1(x, \boldsymbol{\theta}_1)$ as $x \to \infty$, and as a result we that $\lim_{x\to\infty} HR(x; \boldsymbol{\zeta}) = \infty$. □

The behaviour of the hazard rate curves can be spelled out in four different situations.

- Increasing case. This case can happen when $\alpha_i > 1/2$ where $i = 1, 2$. Note that $H_i^{'}(x; \boldsymbol{\theta}_i) > 0$ since the HR function of the GR distribution is an increasing function when its shape parameter $\alpha > 1/2$. On the other hand, Eq.(13) reveals that $H^{'}(x; \boldsymbol{\zeta})$ is positive when the first two terms of this equation dominate the third term. Observe that the third term in Eq.(13) represents the difference between the two hazard rate functions $H_1(x; \boldsymbol{\theta}_1)$ and $H_2(x; \boldsymbol{\theta}_2)$, i.e. $\Delta(H_1, H_2) = |H_1(x; \boldsymbol{\theta}_1) - H_2(x; \boldsymbol{\theta}_2)|$. The value of $\Delta(H_1, H_2)$ became small when the functions $H_1(x; \boldsymbol{\theta}_1)$ and $H_2(x; \boldsymbol{\theta}_2)$ are close from each other, and this can occur when the scale parameters λ_1 and λ_2 are relatively close from each other as well. See Figure 5 (a-c).

- Increasing-decreasing-increasing case. This scenario case can also occur when $\alpha_i > 1/2$ for $i = 1, 2$. It occurs when one of the two HR functions, $H_1(x; \boldsymbol{\theta}_1)$ and $H_2(x; \boldsymbol{\theta}_2)$ dominates the other one substantially after a certain point whereas these functions are close from each other on the beginning. Let $x_\star$ and $x^\star$ be the values at which $H(x; \boldsymbol{\zeta})$ attains its minimum and maximum respectively. Suppose that $H_1(x; \boldsymbol{\theta}_1) > H_2(x; \boldsymbol{\theta}_2)$. On the interval $(0, x^\star)$ the value of $\Delta(H_1, H_2)$ became small and hence is dominated by the first two terms in Eq.(13) which implies that $H^{'}(x; \boldsymbol{\zeta}) > 0$. On the interval $(x^\star, x_\star)$, the value of $\Delta(H_1, H_2)$ became large and therefore dominated the first two terms in Eq(13) implying that

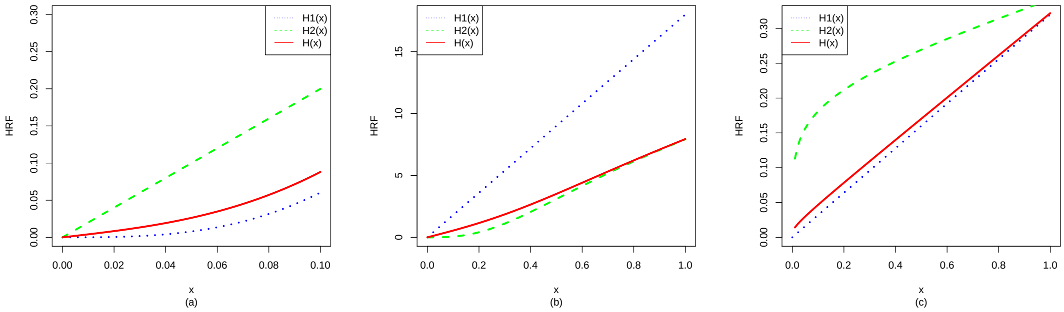

Figure 5: Some plots of the HR curves of the MTGR distribution exhibiting decreasing function for the cases: (a) ($p = 0.8$, $\alpha_1 = 2$, $\alpha_2 = 1$, $\lambda_1 = 1$, $\lambda_2 = 2$); (b) ($p = 0.3$, $\alpha_1 = 1$, $\alpha_2 = 2$, $\lambda_1 = 3$, $\lambda_2 = 2$); (c) ($p = 0.9$, $\alpha_1 = 1$, $\alpha_2 = 0.6$, $\lambda_1 = 0.4$, $\lambda_2 = 0.3$)

$H^{'}(x;\boldsymbol{\zeta}) < 0$. Finally on $(x_{\star}, \infty)$ we have that $H^{'}(x;\boldsymbol{\zeta}) \sim H_i^{'}(x;\boldsymbol{\theta}_i) > 0$ since as $x \to \infty$, $\lim_{x\to\infty} g(x;\boldsymbol{\zeta})q(x;\boldsymbol{\zeta}) = 0$ implying that $H(x;\boldsymbol{\zeta})$ is an increasing function on this interval. See Figure 6(a-c) for further illustration.

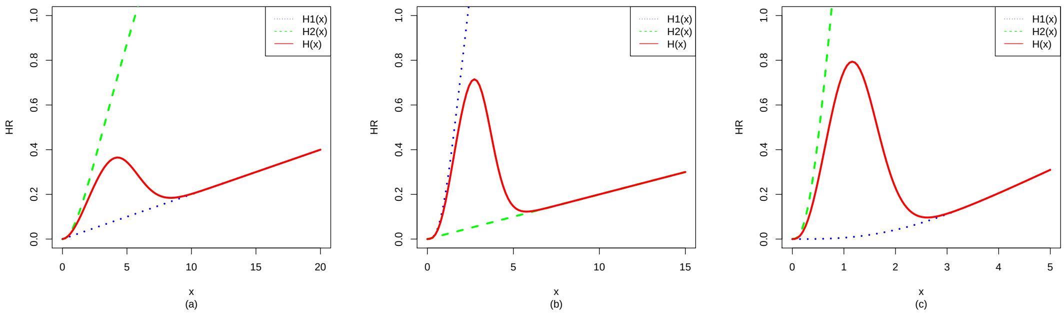

Figure 6: Some plots of the HR curves of the MTGR distribution exhibiting increasing-decreasing-increasing function for the cases: (a) ($p = 0.3$, $\alpha_1 = 1$, $\alpha_2 = 1.5$, $\lambda_1 = 0.1$, $\lambda_2 = 0.3$); (b) ($p = 0.8$, $\alpha_1 = 2$, $\alpha_2 = 1$, $\lambda_1 = 0.5$, $\lambda_2 = 0.1$); (c) ($p = 0.4$, $\alpha_1 = 2$, $\alpha_2 = 1.8$, $\lambda_1 = 0.2$, $\lambda_2 = 1$)

- Bathtub-shaped case. This case can happen when $\alpha_i < \alpha_i < \frac{1}{2}$ or ($\alpha_i < \frac{1}{2}$ and $\alpha_j \geq \frac{1}{2}$), $i \neq j$, $i, j = 1, 2$. When both $H_1(x;\boldsymbol{\theta}_1)$ and $H_2(x;\boldsymbol{\theta}_2)$ have bathtub-shaped HR functions such that their corresponding change points are close from each other, then the HR function of MTGR distribution is a bathtub-shaped. Additionally, when one of these HR functions has an increasing HR that is dominated by the other HR function with a bathtub-shaped HR, then the HR function of the MTGR distribution has a bathtub-shaped HR function with a unique changing point. It is also anticipated that this situation may occur when $\alpha_1 < \alpha_2$ and $\lambda_1 > \lambda_2$ or vice versa, see Figure 7(a-c).

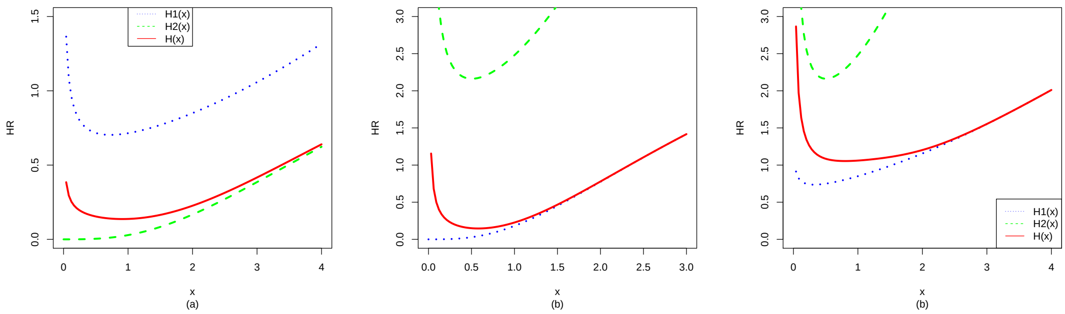

Figure 7: Some plots of the HR curves of the MTGR distribution exhibiting bathtub-shaped hazard rates for the cases: (a) ($p = 0.3$, $\alpha_1 = 0.3$, $\alpha_2 = 2$, $\lambda_1 = 0.4$, $\lambda_2 = 0.3$); (b) ($p = 0.7$, $\alpha_1 = 2$, $\alpha_2 = 0.1$, $\lambda_1 = 0.5$, $\lambda_2 = 1$); (c) ($p = 0.4$, $\alpha_1 = 0.4$, $\alpha_2 = 0.1$, $\lambda_1 = 0.5$, $\lambda_2 = 1$)

- Bi-Bathtub-shaped case. This case can occur also when $\alpha_i < \alpha_i < \frac{1}{2}$ or ($\alpha_i < \frac{1}{2}$ and $\alpha_j \geq \frac{1}{2}$), $i \neq j$, $i, j = 1, 2$. When both $H_1(x; \boldsymbol{\theta}_1)$ and $H_2(x; \boldsymbol{\theta}_2)$ have bathtub-shaped HR functions such that their corresponding change points are far from each other, then the HR function of MTGR distribution is a bi bathtub-shaped HR, see Figure 8(a). Moreover, Additionally, when one of these HR functions has an increasing hazard rate that intersects the other HR function with a bathtub-shaped hazard rate, then the HR of the MTGR distribution has a bi bathtub-shaped with two changing points, see Figure 8(b-c). It is also observed that this situation may occur when $\alpha_1 < \alpha_2$ and $\lambda_1 < \lambda_2$ or vice versa.

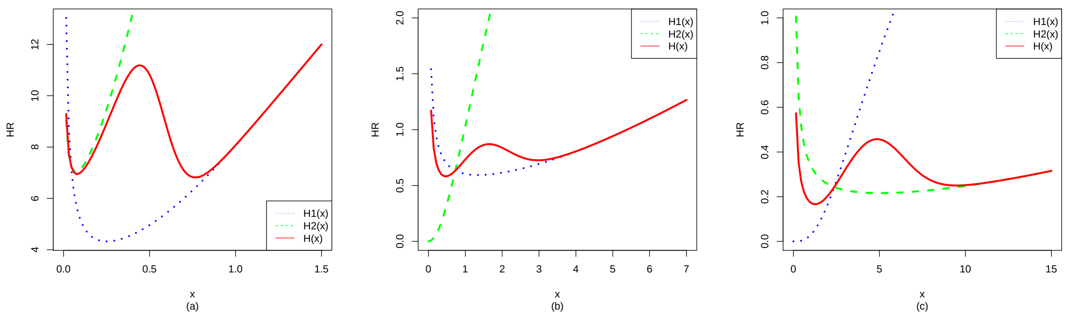

Figure 8: Some plots of the HR curves of the MTGR distribution exhibiting bi-bathtub-shaped hazard rates for the cases: (a) ($p = 0.1$, $\alpha_1 = 0.1$, $\alpha_2 = 0.3$, $\lambda_1 = 2$, $\lambda_2 = 4$); (b) ($p = 0.8$, $\alpha_1 = 0.2$, $\alpha_2 = 1.5$, $\lambda_1 = 0.3$, $\lambda_2 = 0.8$); (c) ($p = 0.3$, $\alpha_1 = 2$, $\alpha_2 = 0.1$, $\lambda_1 = 0.3$, $\lambda_2 = 0.1$)

4 Some statistical properties

In this section, we provide some statistical properties for the proposed model.

4.1 Mean

Let X be a generalized Rayleigh distribution with parameters λ_i and α_i, $i = 1, 2$, i.e., $X \sim \mathrm{GR}(\alpha_i, \lambda_i)$. The k^{th} moments of X can be obtained in view of the result by Choudhury (2005) as

$$E(X^k) = \alpha_i \lambda_i^{-k} \Gamma\left(\frac{k}{2}+1\right)\left[1+\sum_{j=0}^{\infty} a_j (j+1)^{-\frac{k}{2}-1}\right],$$

where $a_j = \frac{(\alpha_i-1)(\alpha_i-2)\ldots(\alpha_i-j)}{j!}(-1)^j$. Therefore, the mean of MTGR distribution is

$$\mu^k = \sum_{i=1}^{2}\left\{p_i \alpha_i \lambda_i^{-k}\Gamma\left(\frac{k}{2}+1\right)\left[1+\sum_{j=0}^{\infty} a_j (j+1)^{-\frac{k}{2}-1},\right]\right\}, \tag{14}$$

where $p_1 = p$ and $p_2 = 1 - p_1$.

4.2 Quantile

The quantile function of the MTGR distribution is the value, say x_q that solves the following non-linear equation

$$p[(1-e^{-\lambda_1^2 x^2})^{\alpha_1}] + (1-p)[(1-e^{-\lambda_2^2 x^2})^{\alpha_2} - (1-q) = 0, \tag{15}$$

where $0 < q < 1$. The median is the value $x_{0.5}$. Note that Eq.(15) can be used to generate random samples from the MTGR distribution.

4.3 Mode

Generally, mode(s) for a distribution play important roles in studying the behaviour of the distribution, particularly in the finite mixture models. Let $k_i(x, \lambda_i) := \exp(-\lambda_i^2 x^2)$. The mode(s) of the MTGR distribution is (are) found by solving the ensuing equation numerically

$$\sum_{i=1}^{2} 2p_i\alpha_i\lambda_i^2 k_i(x,\lambda_i)(1-k_i(x,\lambda_i))^{\alpha_i-2}\left[1-2\lambda_i^2x^2 - k_i(x,\lambda_i)\left(1-2\alpha_i\lambda_i^2x^2\right)\right]$$

Table 1 presents the mean, median and mode of the MTGR distribution by using different choices of the parameters. The results reported in Table 1 reveal many interesting properties of the MTGR distribution. Clearly, the mode is little affected by the changing in the values of the mixing proportion p. Additionally, the mean and the median increase as p increases in the unimodal case, and the mean is always greater than the median. Contrary to the unimodal case, the mean and the median decrease as p increase for the bimodal case, and also, the median is greater than the mean

Table 1: The mean, median and the mode(s)of MTGR distribution for different values of the parameters

$\boldsymbol{\zeta} = (p, \alpha_1, \alpha_2, \lambda_1, \lambda_2)$	Mode(s)	Median	Mean
(0.2,0.3,3,0.1,0.7)	1.6930	1.845891	2.3909
(0.4,0.3,3,0.1,0.7)	1.6870	1.924532	2.9384
(0.6,0.3,3,0.1,0.7)	1.6747	2.06331	3.4859
(0.2,0.9,2,1,2)	0.5180	0.5785	0.6276
(0.4,0.9,2,1,2)	0.5226	0.6105	0.6822
(0.6,0.9,2,1,2)	0.5310	0.6535	0.7369
(0.2, 0.9, 5.0, 0.3, 0.1)	1.2960, 6.8302	6.5675	6.1864
(0.4, 0.9, 5.0, 0.3, 0.1)	1.2956, 6.8296	5.4795	5.0629
(0.6, 0.9, 5.0, 0.3, 0.1)	1.2955, 6.8285	2.6025	3.9394

5 Identifiability of the class of the MTGR distribution

Let $\mathcal{F}_{GR} = \{F_i(x;\boldsymbol{\theta}_i) : i = 1,\dots,m;\ \boldsymbol{\theta}_i \in \mathbb{R}^2_+\}$ be a finite family of cumulative probability distributions spanned by the GR distribution indexed by the vector parameters $\boldsymbol{\theta}_i = (\alpha_i, \lambda_i)$. A finite mixture of the GR distributions of order m can be expressed as a convex combinations of $F_i(x;\boldsymbol{\theta}_i),\dots,F_m(x;\boldsymbol{\theta}_m) \in \mathcal{F}_{GR}$ as

$$F(x;\boldsymbol{\zeta}) = \sum_{k=1}^{m} \omega_i F_i(x;\boldsymbol{\theta}_i), \quad i = 1,\dots,m,$$

where $\omega_i > 0$, called the weights such that $\sum_{i=1}^{m} \omega_i = 1$, and

$$\boldsymbol{\zeta} = (\boldsymbol{\omega}, \boldsymbol{\theta}) = [(\omega_1,\dots,\omega_m), (\boldsymbol{\theta}_1,\dots,\boldsymbol{\theta}_m)].$$

Now, the space of all possible finite mixture densities of the GR distribution denoted by $\mathcal{MTRG}_m$ which can be analytically expressed as

$$\mathcal{MTRG}_m = \left\{ F(x;\boldsymbol{\zeta}) :\ F(x;\boldsymbol{\zeta}) = \sum_{k=1}^{\ell} \omega_i F_i(x;\boldsymbol{\theta}_i);\ F_i(x;\boldsymbol{\theta}_i) \in \mathcal{F}_m;\ \ell \in \{2,\dots,m\} \right\}$$

The identifiability of the finite mixtures is important in statistical inferences, particularly in getting unique and consistent estimates for the indexed parameters of the model. In order to study this problem, we state the definition of the identifiability of a finite mixture. The class $\mathcal{MTRG}_m$ is identifiable if and only if for any arbitrary f and $f^\star \in \mathcal{MTRG}_m$;

$$F = \sum_{k=1}^{m} \omega_i F_i(x;\boldsymbol{\theta}_i) \text{ and } F^\star = \sum_{k=1}^{m^\star} \omega_i^\star F_i^\star(x;\boldsymbol{\theta}_i) \text{ such that } F = F^\star \text{ implies that } m = m^\star,$$

and $(\omega_1, F_1), \ldots, (\omega_m, F_m)$ are the permutations of $(\omega_1^\star, F_1^\star), \ldots, (\omega_m^\star, F_m^\star)$. It is clear that showing the identifiability for certain finite mixture models is quite difficult and is not straightforward by using the definition. Therefore, several authors have contributed in providing conditions for establishing the identifiability of various finite mixture models. Related to this topic, readers are referred to Teicher (1963); Chandra (1977); Al-Hussaini and Ahmad (1981); Ahmad (1988); Ahmad and Abd-El-Hakim (1990); Atienza et al. (2006), among others. In this paper, we show the identifiability of the family of MTGR distributions using the results given in Atienza et al. (2006).

Theorem 5.1. *Atienza et al. (2006) Let $\mathcal{F}$ be a class of cumulative probability distributions. Let $M : F_i \longrightarrow \varphi_i$ be a linear mapping which transforms any $F_i \in \mathcal{F}$ into a real function with domain $S_{\psi_i}(F) \in \mathbb{R}^d$. Let $S_0(F) = \{t \in S_\varphi(F) : \varphi_F(t) \neq 0\}$. Suppose that there exists a total order $\preceq$ on $\in \mathcal{F}$ such that for any $F \in \mathcal{F}$ there exists a point $t(F) \in S_0^{'}(F)$, where $A^{'}$ denotes the closure of the set A satisfying*

i *For $F_1, \ldots, F_m \in \mathcal{F}$ such that $F_1 < F_i$ for $2 \le i \le m$, then $t(F) \in [S_0(F_1) \cap [\cap_{i=2}^m S_\varphi(F_i)]^{'}$,*

ii *for each $F_1, F_2 \in \mathcal{F}$, such that $F_1 < F_2$ then*

$$\lim_{t \to t(F_1)} \frac{\varphi_2(t)}{\varphi_1(t)} = 0,$$

Then the class G of all finite mixing distributions is identifiable relative to $\mathcal{F}$.

Note that the linear mapping in the above theorem can be taken as the moment generating function of a random variable X; $E(\exp(tx))$ or the real moments $E(X^t) = E(\exp(t\ln(x)))$. It has been observed that these choices have been used by several authors, see for example Otiniano et al. (2015) and Otiniano et al. (2017). In this paper, we use the moment generating function of $2t\ln(X)$ of the GR distribution as the linear mapping in order to establish the identifiability of the finite mixtures of the GR distribution.

Theorem 5.2. *The family $\mathcal{MTRG}_{GR}$ of all finite mixtures of $\mathcal{F}_{GR}$ is identifiable.*

Proof. Let M be the map which transform a distribution function $F \in \mathcal{F}_{GR}$ into the moment generating function of $2t\ln(X)$, where X is the random variable following the GR distribution with parameters α_i and λ_i. The moment generating function of $2t\ln(X)$ after simple algebra lead to

$$M[F(.;\lambda,\alpha)] = \varphi_F(t) = \frac{\Gamma(\alpha+1)\Gamma\left(1-\frac{t}{\lambda^2}\right)}{\Gamma\left(\alpha+1-\frac{t}{\lambda^2}\right)}, \qquad t \in (-\infty,\, \lambda^2) \tag{16}$$

It is clear from Eq.(16) that $S_0(F(.;\lambda,\alpha)) = (-\infty,\, \lambda^2)$. Now, let $F_1,\ F_2 \in \mathcal{F}_{GR}$, then we have total order in $\mathcal{F}_{GR}$; $F_1 < F_2$ when the following cases hold

- $\lambda_1 < \lambda_2$ and $\alpha_1 = \alpha_2$
- $\lambda_1 = \lambda_2$ and $\alpha_1 > \alpha_2$

To verify the sufficiency condition in Theorem 5.1, consider the case $\lambda_1 < \lambda_2$ and $\alpha_1 = \alpha_2$. In this case we have that $t(F_1) = \lambda_1^2$ which satisfies $t(F_1) = \lambda_1^2 \in [S_0(F_1) \cap S_\varphi(F_2)]'$. Once the total order is established, it remains to show that the following limit goes to 0 as $t \to \lambda_1^2$.

$$\lim_{t\to\lambda_1^2} \frac{\varphi_{F_2(t)}}{\varphi_{F_1}(t)} = \lim_{t\to\lambda_1^2} \left\{ \rho(t;\alpha,\lambda_1,\lambda_2) \frac{\Gamma\left(1-\frac{t}{\lambda_2^2}\right)}{\Gamma\left(1-\frac{t}{\lambda_1^2}\right)} \right\}$$

where

$$\rho(t;\alpha,\lambda_1,\lambda_2) = \frac{\Gamma\left(\alpha+1-\frac{t}{\lambda_2^2}\right)}{\Gamma\left(\alpha+1-\frac{t}{\lambda_1^2}\right)},$$

and that

$$\lim_{t\to\lambda_1^2} \rho(t;\alpha,\lambda_1,\lambda_2) = \frac{\Gamma\left(\alpha+1-\frac{\lambda_1^2}{\lambda_2^2}\right)}{\Gamma(\alpha)} > 0. \tag{17}$$

due to the fact that $\lambda_1^2/\lambda_2^2 < 1$. Now observe that

$$\lim_{t\to\lambda_1^2} \Gamma\left(1-\frac{t}{\lambda_1^2}\right) = \Gamma(0+) = \infty, \tag{18}$$

see Abramowitz (1965). With $\lambda_1^2 < \lambda_2^2$, we have that

$$\lim_{t\to\lambda_1^2} \Gamma\left(1-\frac{t}{\lambda_1^2}\right) = \Gamma\left(1-\frac{\lambda_1^2}{\lambda_2^2}\right) > 0. \tag{19}$$

On using Eqns. (17), (18), and (19), we have

$$\lim_{t\to\lambda_1^2} \frac{\varphi_{F_2(t)}}{\varphi_{F_1}(t)} = 0.$$

The second case can be proved similarly, which completes the proof. □

6 Estimation parameters of MTGR distribution

This section deals with the estimation of unknown parameters of the model using frequentist and Bayesian methods under Type-I censored data. Toward this goal, suppose that the lifetime data say the random variable X, follows an MTGR$(p,\alpha,\alpha,\lambda_1,\lambda_2)$ distribution with PDF and CDF given by Eqns.(6) and (7) respectively. Assume that the total r number of units with lifetimes, say $\boldsymbol{x} = (x_{11}, x_{12}, \ldots, x_{1r_1}, x_{21}, x_{22}, \ldots, x_{2r_2})$ are observed till the prefixed time T reaches in which the r_1 number of units follow GR distribution with parameters α, λ_1, and r_2 number of units follow GR distribution with parameters α and λ_2 such that $r = (r_1 + r_2)$. Note that we assume that the lifetime distribution for the r_1 and r_2 units follow GR distribution with common shape parameters but with different scale parameters due to identifiability problems, and hence consistency of the ML estimates can be achieved. Therefore, the lifetimes of the total $(n-r)$ number of units are not observed. Now the likelihood function of $(\alpha, \lambda_1, \lambda_2, p \mid \boldsymbol{x})$ can be written as

$$
\begin{aligned}
L(\alpha, \lambda_1, \lambda_2, p \mid \boldsymbol{x}) \propto \Big\{ \prod_{k=1}^{r_1} p f_1(x_{k1}; \alpha, \lambda_1) \Big\} \Big\{ \prod_{k=1}^{r_2} (1-p) f_2(x_{k2}; \alpha, \lambda_2) \Big\} \\
\times \big[1 - F(T; \alpha, \lambda_1, \lambda_2)\big]^{n-r}. \qquad (20)
\end{aligned}
$$

$$
\propto \quad p^{r_1} (1-p)^{r_2} \alpha^r \eta_1 \eta_2 \Delta_1 \Delta_2 \Lambda \prod_{j=1}^{r_1} x_{1j} \cdot \prod_{j=1}^{r_2} x_{2j}
$$

where $r = r_1 + r_2$ and

$$
\begin{aligned}
\eta_i &= \lambda_i^{2r_i} e^{-\sum_{j=1}^{r_i} (\lambda_i x_{ij})^2} \\
\Delta_i &= \prod_{j=1}^{r_i} \big(1 - e^{-(\lambda_i x_{ij})^2}\big)^{\alpha-1}, \quad \text{for} \quad i = 1, 2.
\end{aligned}
$$

$$
\text{and} \quad \Lambda = \Big\{1 - \big\{p\big(1 - e^{-(\lambda_1 T)^2}\big)^{\alpha} + (1-p)\big(1 - e^{-(\lambda_2 T)^2}\big)^{\alpha}\big\}\Big\}^{n-r}
$$

6.1 Maximum Likelihood Estimation

The maximum likelihood (ML) method is a popular method used to estimate unknown parameters due to its desirable properties, including consistency, asymptotic efficiency, and invariance. The ML estimates for the parameters can be obtained by maximizing the likelihood function over the parameter space. Equivalently, these estimates can be obtained based on the log-likelihood function. To do so, let $l = \ln L(\alpha, \lambda_1, \lambda_2, p \mid \boldsymbol{x})$, then the partial derivatives with respect to p, α, λ_i are given by

$$
\begin{aligned}
\frac{\partial l}{\partial p} &= \frac{r_1}{p} - \frac{r_2}{1-p} - \frac{n-r}{1-F(T)} [F_1(T) - F_2(T)], \\
\frac{\partial l}{\partial \alpha} &= \frac{r}{\alpha} + \sum_{j=1}^{r_1} \ln A_1(x_j) + \sum_{j=1}^{r_2} \ln A_2(x_j), \\
&- \frac{n-r}{1-F(T)} \big[p F_1(T) \ln A_1(T) + (1-p) F_2(T) \ln A_1(T)\big], \\
\frac{\partial l}{\partial \lambda_i} &= \frac{2r_i}{\lambda_i} - 2\lambda_i \sum_{j=1}^{r_i} x_{ij}^2 + 2(\alpha-1)\lambda_i \sum_{j=1}^{r_i} \frac{x_{ij}^2 e^{-(\lambda_i x_{ij})^2}}{A_i(x_{ij})} - \frac{p(n-r)T}{\lambda_i(1-F(T))} f_i(T),
\end{aligned}
$$

where $i = 1, 2$ and $A_i(x) = 1 - e^{-(\lambda_i x)^2}$. Further we denote $f_i = f_i(x; \alpha, \lambda_i)$ and $F(x) = F(x; \alpha, \lambda_1, \lambda_2)$. Solving simultaneously all the above equations, we can get the maximum likelihood estimators for α, λ_i, p. Since the estimators do not turn out to have a closed form, so a numerical technique such as the Newton-Raphson method is applied to compute maximum likelihood estimates of p, α, λ_i, respectively, denoted as $\hat{p}, \hat{\alpha}, \hat{\lambda}_i$.

For interval estimation of $\phi = (p, \lambda_1, \lambda_2, \alpha)$, we derive the observed information matrix, since the form of the expected information matrix is very complicated and requires numerical integration. The elements of the 4×4 observed information matrix; $\mathbf{I}(\phi) = E(\frac{\partial^2 l}{\partial\phi\partial\phi^t})$ are given in the Appendix. Under some regularity conditions for unknown parameters in the interior of parameter space but not on the boundaries, the asymptotic distribution of $\sqrt{n}\left(\hat{\phi} - \phi\right)$ follows multivariate normal with mean vector zero and variance-covariance matrix is $J^{-1}(\phi)$ i.e., $\sqrt{n}\left(\hat{\phi} - \phi\right) \sim N_4\left(0, J^{-1}(\phi)\right)$, where $J(\phi)$ is the expected information matrix. The asymptotic behavior is valid if $J(\phi)$ is replaced by $I\left(\hat{\phi}\right)$, i.e., the observed information matrix evaluated at $\hat{\phi}$. Thus, the multivariate normal $N_4\left(0, I^{-1}\left(\hat{\phi}\right)\right)$ distribution can be used to obtain approximate confidence intervals for the considered parameters.

6.2 Bootstrap confidence intervals

In this section, we use the bootstrap technique to construct confidence intervals for the unknown parameters of the model. Here, we consider two methods of bootstrap CIs, namely, bootstrap-t (Boot-t) and Bootstrap-p (Boot-p), see for example, Efron and Tibshirani (1994). The following steps are required for the Boot-p method:

1. Draw sample $\boldsymbol{x} = (x_{11}, x_{12}, \ldots, x_{1r_1}, x_{21}, x_{22}, \ldots, x_{2r_2})$ from $GR(x; \alpha, \lambda_1, \lambda_2)$ corresponding to the values of, say $\theta = (\alpha, \lambda_1, \lambda_2, p), n$ and T. From the drawn sample, compute the estimate of θ, say $\hat{\theta}$.

2. Next draw a bootstrap sample of $\boldsymbol{x} = (x^*_{11}, x^*_{12}, \ldots, x^*_{1r_1}, x^*_{21}, x^*_{22}, \ldots, x^*_{2r_2})$ from $GR(x; \hat{\theta}^*)$, and compute the updated bootstrap estimate of θ say $\hat{\theta}^*$.

3. Repeat the previous step, say M times.

4. Let $\hat{F}(x) = P(\hat{\theta}^* \leq x)$, be the CDF of $\hat{\theta}^*$. Then define $\hat{\theta}_{Boot-p}(x) = F^{-1}(x)$ for a given x. Therefore the approximate $100(1-\gamma)\%$ confidence interval for θ is now given by $\Big(\hat{\theta}_{Boot-p}(\frac{\gamma}{2}),$
$\hat{\theta}_{Boot-p}(1 - \frac{\gamma}{2})\Big)$

The following steps are required to construct bootstrap confidence intervals using the Boot-t Method:

1. Draw sample $\boldsymbol{x} = (x_{11}, x_{12}, \ldots, x_{1r_1}, x_{21}, x_{22}, \ldots, x_{2r_2})$ from $GR(x; \alpha, \lambda_1, \lambda_2)$ corresponding to the values of, say $\theta = (\alpha, \lambda_1, \lambda_2, p), n$ and T. From the drawn sample, compute the estimate of θ, say $\hat{\theta}$.

2. Next draw a bootstrap sample of $\boldsymbol{x} = (x^*_{11}, x^*_{12}, \ldots, x^*_{1r_1}, x^*_{21}, x^*_{22}, \ldots, x^*_{2r_2})$ from $GR(x; \hat{\theta}^*)$, and compute the updated bootstrap estimate of θ, say $\hat{\theta}^*$ and $\hat{V}(\hat{\theta}^*)$.

3. compute the statistic T^* defined as $T^* = \left(\hat{\theta}^* - \hat{\theta}\right)/\sqrt{\hat{V}(\hat{\theta}^*)}$

4. Repeat the steps 2 and 3, say M times.

5. Let $\hat{F}(x) = P(T^* \leq x)$, be the CDF of $\hat{\theta}^*$. Define $\hat{\theta}_{Boot-t}(x) = \hat{\theta} + \sqrt{\hat{V}(\hat{\theta}^*)}\hat{F}^{-1}(x)$ for a given x. Then the approximate $100(1-\gamma)\%$ confidence interval for θ is obtained as $\left(\hat{\theta}_{Boot-t}(\frac{\gamma}{2}), \hat{\theta}_{Boot-t}(1-\frac{\gamma}{2})\right)$

6.3 Bayesian Estimation

Bayesian inference procedures have been taken into consideration by many statistical researchers, especially researchers in the field of survival analysis and reliability engineering. In this section, the Bayes estimates of model parameters $\alpha, \lambda_1, \lambda_2$ and p are obtained under the square error loss (SEL) function. We consider two prior distributions for the parameters of MTGR distribution. In each case, we provide Bayesian estimator under the SEL function.

6.3.1 Bayes estimators under uniform priors based on SEL function

We assume that the parameters $\alpha, \lambda_1, \lambda_2$ and p of MTGR distribution have independent uniform prior distributions as given by

$$\alpha \sim U(0,\infty),\ \lambda_1 \sim U(0,\infty),\ \lambda_1 \sim U(0,\infty),\ \text{and } p \sim U(0,1),$$

Hence, the joint prior density function is formulated as follows:

$$\pi_1(\alpha, \lambda_1, \lambda_2, p) \propto 1;\ \alpha, \lambda_1, \lambda_2 > 0,\ 0 < p < 1. \tag{21}$$

The joint posterior distribution in terms of a given likelihood function in Eq.(20) and joint prior distribution $\pi_1(\alpha, \lambda_1, \lambda_2, p)$ in Eq.(21) is defined as

$$\pi_1^*(\alpha, \lambda_1, \lambda_2, p \mid data) \propto L(data)\ \pi_1(\alpha, \lambda_1, \lambda_2, p)$$

Hence, the joint posterior density of parameters $\alpha, \lambda_1, \lambda_2$ and p based on Type-I censored data is given by

$$\pi_1^*(\alpha, \lambda_1, \lambda_2, p \mid x) = K_1\ p^{r_1}(1-p)^{r_2}\alpha^r \eta_1\eta_2\Delta_1\Delta_2\Lambda. \tag{22}$$

where K_1 is given as

$$K_1^{-1} = \int_0^1 \int_0^\infty \int_0^\infty \int_0^\infty p^{r_1}(1-p)^{r_2}\alpha^r \eta_1\eta_2\Delta_1\Delta_2\Lambda\ d\lambda_1 d\lambda_2 d\alpha dp.$$

Under the SEL function, the Bayes estimate of a parameter is equal to its posterior mean. Note that estimators using other loss functions can be obtained similarly. From Eq. (22), it is clear that the Bayes estimators of $\alpha, \lambda_1, \lambda_2$ and p can not be explicitly obtained due to the involvement of the ratio of multiple integrals, therefore, we use the Markov chain Monte Carlo (MCMC) technique to obtain the desired estimates.

6.3.2 Bayes estimators under the beta and gamma priors based on SEL function

Here, we assume that the parameters $\alpha, \lambda_1, \lambda_2$ and p of MTGR distribution have independent beta and gamma prior distributions as given by

$$p \sim \text{Beta}(a, b), \lambda_1 \sim \text{Gamma}(c, d), \lambda_2 \sim \text{Gamma}(e, f), \alpha \sim \text{Gamma}(g, h).$$

where a, b, c, d, e, f, g and h are positive constants. Here, the joint prior density function is formulated as follows:

$$\pi_2(\alpha, \lambda_1, \lambda_2, p) \propto p^{a-1}(1-p)^{b-1}\lambda_1^{c-1}\lambda_2^{e-1}\alpha^{g-1}e^{-(d\lambda_1+f\lambda_2+h\alpha)} \tag{23}$$

Hence, the joint posterior density of parameters $\alpha, \lambda_1, \lambda_2andp$ under joint prior density $\pi_2(\alpha, \lambda_1, \lambda_2, p)$ for the Type-I censored data is given by

$$\pi_2^*(\alpha, \lambda_1, \lambda_2, p \mid x) \propto p^{r_1+a-1}(1-p)^{r_2+b-1}\lambda_1^{c-1}\lambda_2^{e-1}\alpha^{r+g-1}e^{-(d\lambda_1+f\lambda_2+h\alpha)} \prod_{j=1}^{r_1} x_{1j} \prod_{j=1}^{r_2} x_{2j}\eta_1\eta_2\Delta_1\Delta_2\Lambda. \tag{24}$$

From Eq.(24), it is clear that the Bayes estimators of $\alpha, \lambda_1, \lambda_2$ and p can not be obtained explicitly, hence, we use Markov chain Monte Carlo (MCMC) technique to obtain the desired estimates.

6.3.3 MCMC Method

To obtain the Bayes estimates of the parameters $\alpha, \lambda_1, \lambda_2$ and p under type-I censoring, samples are generated from the posterior distribution. From Eq.(22), the conditional posterior distributions for the parameters $\alpha, \lambda_1, \lambda_2$ and p under uniform prior are, respectively given by

$$\begin{aligned}
\pi_1^*(\alpha \mid \lambda_1, \lambda_2, p, x) &= \alpha_1^r\Delta_1\Delta_2\Lambda, \\
\pi_1^*(\lambda_1 \mid \alpha, \lambda_2, p, x) &= \eta_1\Delta_1\Lambda, \\
\pi_1^*(\lambda_2 \mid \alpha, \lambda_1, p, x) &= \eta_2\Delta_2\Lambda, \\
\pi_1^*(p \mid \alpha, \lambda_1, \lambda_2, x) &= p^{r_1}(1-p)^{r_2}\Lambda.
\end{aligned} \tag{25}$$

From Eq.(24), the conditional posterior distributions for the parameters $\alpha, \lambda_1, \lambda_2$ and p under beta andgamma priors are, respectively given by

$$\begin{aligned}
\pi_2^*(\alpha \mid \lambda_1, \lambda_2, p, x) &= \alpha^{r+g-1}\ e^{-h\alpha}\ \Delta_1\Delta_2\Lambda, \\
\pi_2^*(\lambda_1 \mid \alpha, \lambda_2, p, x) &= \lambda_1^{c-1}\ e^{-d\lambda_1}\ \eta_1\Delta_1\Lambda, \\
\pi_2^*(\lambda_2 \mid \alpha, \lambda_1, p, x) &= \lambda_2^{e-1}\ e^{-f\lambda_2}\ \eta_2\Delta_2\Lambda, \\
\pi_2^*(p \mid \alpha, \lambda_1, \lambda_2, x) &= p^{r_1+a-1}(1-p)^{r_2+b-1}\Lambda.
\end{aligned} \tag{26}$$

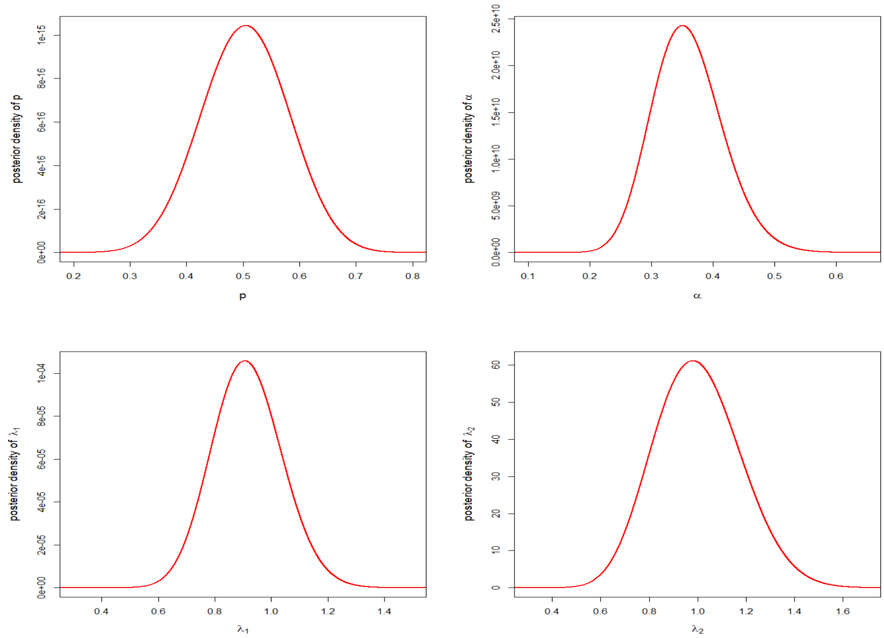

Figure 9: The posterior density of α, λ_1, λ_2 and p under uniform prior.

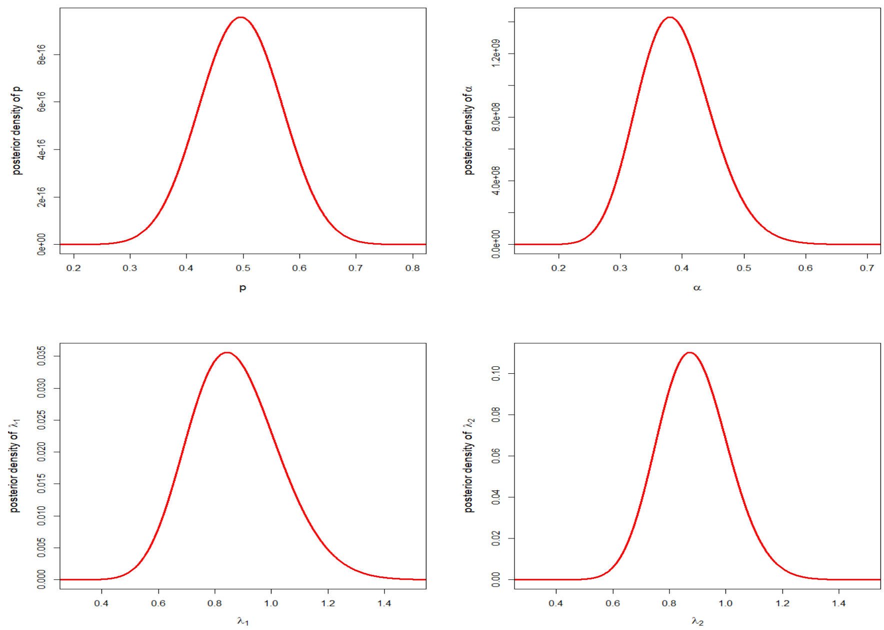

Figure 10: The posterior density of α, λ_1, λ_2 and p under beta-gamma prior.

Since the conditional posterior distributions of the parameters $\alpha,\ \lambda_1,\ \lambda_2$ and p are not reducible into the forms of some well-known distributions, and we use Metropolis-Hastings algorithm proposed by Metropolis et al. (1953) and Hastings (1970) to generate posterior samples. If the conditional posterior distributions of the parameters are unimodal and are roughly symmetric, then these can be approximated by a normal distribution. Figures 9 and 10 show that the conditional distributions of $\alpha,\ \lambda_1,\ \lambda_2$ and p are unimodal and very much symmetric by visual inspection. Therefore, to generate random samples from these conditional distributions, we use the following steps from the Metropolis-Hastings algorithm:

- Set initial guesses for the parameters $(\alpha, \lambda_1, \lambda_2, p)$ as $(\alpha^0, \lambda_1^0, \lambda_2^0, p^0)$.
- Set $i = 1$.
- Generate $\alpha \sim N(\alpha^{i-1}, \sigma_{11}), \lambda_1 \sim N(\lambda_1^{i-1}, \sigma_{22}), \lambda_2 \sim N(\lambda_2^{i-1}, \sigma_{33})$ and $p \sim N(p_{i-1}, \sigma_{44})$, where σ_{ii} denotes the $(i,i)th$ entry of the variance-covariance matrix Σ.
- Compute $q = \frac{\pi^*(\alpha^i, \lambda_1^i, \lambda_2^i, p^i|x)}{\pi^*(\alpha^{i-1}, \lambda_1^{i-1}, \lambda_2^{i-1}, p^{i-1}|x)}$.
- Accept $(\alpha^i, \lambda_1^i, \lambda_2^i, p^i)$ with the probability $\min(1, q)$.
- Repeat Steps 3–5 M times to obtain M number of samples for the parameters $(\alpha, \lambda_1, \lambda_2, p)$.
- Obtain the Bayes estimates using MCMC under SEL function as

$$\tilde{p}_{MC} = \frac{1}{M'} \sum_{i+1}^{M'} p^{(i)}, \quad \tilde{\alpha}_{MC} = \frac{1}{M'} \sum_{i=1}^{M'} \alpha^{(i)}, \qquad \tilde{\lambda}_{j\,MC} = \frac{1}{M'} \sum_{i=1}^{M'} \lambda_j^{(i)}, \text{for } j = 1, 2$$

  where $M' = M - M_0$ and M_0 is the count of burns in period.

- . The $100(1-\delta)\%$ HPD credible intervals are obtained using the idea of Chen and Shao (1999).

7 Numerical Illustration

In this section, we provide some simulation results based on maximum likelihood and Bayesian methods. First, we consider the performance of the MLEs of the parameters with respect to sample size n and for different parameter values for the MTGR distribution. Let $\hat{p}$, $\hat{\alpha}$ $\hat{\lambda}_1$ and $\hat{\lambda}_2$ be the MLEs of the parameters p, α, λ_1 and λ_2, respectively. We calculate the mean squared errors (MSEs) and average bias (ABs) of the MLEs of the parameters p, α, λ_1 and λ_2 based on simulation results of 1000 replications. Results of the simulation study are summarized in Table 3 for different values of n, p, α, λ_1 and λ_2. From Table 3, we observe that as sample size increases, the average biases and the MSEs decrease. It verifies the consistency properties of MLEs. In Table 4, we have reported average confidence Length(ACL) along with coverage probabilities of the parameters of the model. The boot-p and boot-t confidence intervals for the parameters of the model are presented in Tables 4 and 5. On comparing the various interval estimates, we observe that the HPD interval estimates are better in terms of interval lengths for the two sets of parameters. We also observe that except for parameter α, the results get better when the value of T increases. We further observe that the interval lengths get smaller with the increase in the sample size. Next, we assess the performance of the Bayes estimates in terms of their mean squared errors (MSEs) and average biases (ABs) based on Monte Carlo simulation. Bayes estimates are obtained using uniform priors (Prior-I) and beta and gamma priors (Prior-II) under the SEL function. We generated sample of sizes $n = 35, 50$ and 70 from the MTGR distribution with parameters p, α, λ_1 and λ_2 such that $(p, \alpha, \lambda_1, \lambda_2) \in \{(0.5, 0.5, 0.5, 0.6), (0.65, 0.5, 0.6, 0.4)\}$. The considered hyperparameter values are shown in Table 2 and the hyperparameters value are considered in such a way that the mean of prior density is equal to the corresponding model parameter value. Also, we have computed Bayes HPD credible length and coverage probabilities (CPs) of the parameters p, α, λ_1 and λ_2. Results of the simulation study are summarized in Tables 6-9. It is evident from these tables that as the sample size increases, the MSEs of the Bayes estimates decrease, which verifies the consistency properties of the estimators. For the sake of comparison purposes, if we compare MLEs with Bayes estimates in terms of MSEs, we observe that Bayes estimates perform marginally better than MLEs in almost all cases. Further, comparing the choice of priors, Prior-I performs better marginally better than Prior-II in terms of MSEs for the parameters p and α while Prior-II performs better than Prior-I for the parameters λ_1 and λ_2. It is also observed that HPD credible intervals have smaller interval lengths than the intervals obtained by using the asymptotic normality property of MLEs. Besides, boot-p performs better than boot-t in terms of interval lengths and coverage probabilities.

Table 2: Hyperparameters value for Prior-II corresponding two sets of parameters p, α, λ_1 and λ_2.

Parameter	Hyperparameter
$p = 0.5,\ \lambda_1 = 0.5,\ \lambda_2 = 0.6, \alpha = 0.5,$	$(a, b) = (1, 1),\ (c, d) = (1, 2)$
	$(e, f) = (3, 5),\ (g, h) = (1, 2)$
$p = 0.65,\ \lambda_1 = 0.6,\ \lambda_2 = 0.4,\ \alpha = 0.5,$	$(a, b) = (13, 7),\ (c, d) = (3, 5)$
	$(e, f) = (2, 5),\ (g, h) = (1, 2)$

8 Real data Analysis

In this section, to show the applicability of the methodology presented in this article, we present two real data sets for the illustration purpose.

Table 3: MSEs and ABs of the MLEs for the parameters p, α, λ_1 and λ_2.

$(p, \alpha, \lambda_1, \lambda_2)$	n	T	$\hat{p}$	$\hat{\alpha}$	$\hat{\lambda_1}$	$\hat{\lambda_2}$
(0.5, 0.5,0.5 0.6)	35	1	0.20177	0.09687	0.22088	0.11875
			-0.31071	-0.14495	0.30563	0.14501
		1.25	0.10253	0.08638	0.17654	0.08964
			-0.21779	0.12022	0.24773	0.14216
		1.5	0.08287	0.061635	0.12289	0.08013
			-0.10036	0.07623	0.22219	0.04389
	50	1	0.01763	0.03879	0.21551	0.08645
			-0.02645	-0.14295	0.23688	0.14095
		1.25	0.01458	0.02955	0.16711	0.07242
			-0.01884	0.11968	0.21420	0.14984
		1.5	0.01373	0.02667	0.11006	0.06730
			-0.01740	0.06199	0.21368	0.02957
	70	1	0.01574	0.03132	0.17316	0.04567
			-0.01584	-0.13573	0.14644	0.13424
		1.25	0.01295	0.01997	0.15990	0.04001
			-0.01247	0.06300	0.12703	0.12162
		1.5	0.01141	0.01369	0.10117	0.03366
			-0.01244	0.05227	0.10502	0.03007
(0.65,0.5,0.6,0.4)	35	1	0.10655	0.11427	0.18417	0.23134
			-0.04376	-0.18315	0.26246	-0.25636
		1.5	0.10645	0.11038	0.11195	0.19338
			-0.03425	0.08191	0.24665	0.20683
		1.7	0.10223	0.02544	0.09699	0.19232
			-0.02634	0.07315	0.22098	0.18430
	50	1	0.04491	0.11358	0.13033	0.14453
			-0.04309	-0.09451	0.25610	-0.17311
		1.5	0.02494	0.05809	0.08115	0.14121
			-0.03405	0.06675	0.20557	0.14719
		1.7	0.02422	0.01474	0.07934	0.12558
			-0.02381	0.05027	0.20632	0.11367
	70	1	0.04429	0.03263	0.10803	0.13964
			-0.03931	-0.09171	0.15857	-0.16719
		1.5	0.02387	0.02297	0.07744	0.13185
			-0.03113	0.04862	0.20164	0.14469
		1.7	0.02350	0.00995	0.07737	0.12017
			-0.02257	0.04552	0.20603	0.10889

Table 4: The average confidence Length(ACL), Boot-p and Boot-t confidence interval length and CP for the parameters $p = 0.5, \alpha = 0.5, \lambda_1 = 0.5$ and $\lambda_2 = 0.6$.

		ACI				Boot-p				Boot-t			
n	T	p	α	λ_1	λ_2	p	α	λ_1	λ_2	p	α	λ_1	λ_2
35	1	0.41197	0.42728	0.89719	0.75502	0.22202	0.30941	0.442421	0.60229	2.23882	3.20588	1.93069	3.51295
		0.923	0.929	0.899	0.851	0.991	0.695	0.843	0.952	0.747	0.699	0.945	0.647
	1.25	0.37821	0.45076	0.88196	0.73623	0.24772	0.37418	0.41631	0.50394	2.73124	3.27811	1.90952	2.73479
		0.966	0.879	0.988	0.899	0.850	0.838	0.848	0.938	0.793	0.850	0.949	0.974
	1.5	0.35538	0.48492	0.84307	0.70410	0.26520	0.48042	0.38492	0.444505	3.11055	3.38963	1.90952	2.32636
		0.887	0.991	0.893	0.979	0.932	0.840	0.838	0.742	0.989	0.926	0.843	0.749
50	1	0.34453	0.34982	0.75127	0.63231	0.18558	0.30155	0.36378	0.50677	2.11348	3.18847	1.88015	3.29579
		0.977	0.919	0.988	0.936	0.997	0.866	0.846	0.957	0.945	0.877	0.846	0.948
	1.25	0.31773	0.37495	0.73077	0.61901	0.20739	0.30238	0.33981	0.41097	2.71790	3.26669	1.85075	2.59430
		0.978	0.899	0.891	0.913	0.993	0.643	0.845	0.836	0.992	0.910	0.899	0.756
	1.5	0.29924	0.39225	0.70226	0.59212	0.22284	0.349469	0.31309	0.43023	3.08874	3.37909	1.85017	2.17445
		0.899	0.919	0.993	0.919	0.955	0.840	0.837	0.925	0.967	0.910	0.819	0.819
70	1	0.29116	0.29275	0.63283	0.53665	0.15368	0.23622	0.30727	0.42727	2.18112	3.18691	1.83679	2.56508
		0.988	0.698	0.798	0.991	0.998	0.630	0.729	0.776	0.874	0.958	0.837	0.966
	1.25	0.26816	0.31075	0.61179	0.52462	0.17386	0.27136	0.28074	0.34987	2.68200	3.21165	1.80961	2.17708
		0.995	0.887	0.883	0.963	0.999	0.692	0.843	0.939	0.993	0.855	0.910	0.889
	1.5	0.25345	0.32362	0.58771	0.50565	0.18763	0.29926	0.26064	0.28698	3.05323	3.26706	1.79065	2.11670
		0.911	0.877	0.881	0.911	0.951	0.943	0.749	0.842	0.933	0.861	0.944	0.929

Table 5: The average confidence Length(ACL), Boot-p and Boot-t confidence interval length and CP for the parameters $p = 0.65, \alpha = 0.5, \lambda_1 = 0.6$ and $\lambda_2 = 0.4$.

		ACI				Boot-p				Boot-t			
n	T	p	α	λ_1	λ_2	p	α	λ_1	λ_2	p	α	λ_1	λ_2
35	1	0.42811	0.40091	0.88566	0.68067	0.22985	0.22344	0.34140	0.64433	2.39312	3.29689	1.61608	3.82204
		0.899	0.937	0.938	0.848	0.990	0.673	0.849	0.892	0.797	0.766	0.683	0.885
	1.5	0.34372	0.47465	0.79301	0.64151	0.25196	0.36847	0.28967	0.62399	3.11466	3.38455	1.50923	3.59534
		1.000	0.991	0.983	0.983	0.993	0.885	0.792	0.985	0.990	0.992	0.789	0.991
	1.7	0.32767	0.48035	0.72556	0.54427	0.25980	0.44764	0.28335	0.61442	3.34443	3.53956	1.50655	3.23503
		0.899	0.969	0.991	0.987	0.990	0.977	0.865	0.981	0.990	0.998	0.992	0.876
50	1	0.35501	0.32600	0.73814	0.56361	0.19562	0.19424	0.27556	0.54235	2.29210	3.29707	1.57877	3.53276
		0.878	0.899	0.988	0.960	0.899	0.659	0.693	0.924	0.991	0.778	0.883	0.765
	1.5	0.28822	0.37312	0.65907	0.53883	0.21037	0.31762	0.23684	0.51711	3.10881	3.36612	1.50780	3.37089
		1.000	0.925	0.838	0.673	0.957	0.890	0.696	0.861	0.991	0.895	0.936	0.991
	1.7	0.27543	0.38204	0.60606	0.46089	0.21499	0.35904	0.23086	0.49358	3.252221	3.50206	1.46736	3.21411
		0.984	0.892	0.988	0.987	1.000	0.875	0.993	0.986	0.877	0.998	0.939	0.956
70	1	0.29927	0.27319	0.62253	0.46521	0.18229	0.15393	0.22805	0.45977	2.22891	3.26534	1.53451	3.46884
		0.998	0.985	0.938	0.734	0.915	0.763	0.893	0.878	0.896	0.759	0.881	0.881
	1.5	0.24463	0.31126	0.55664	0.45091	0.17683	0.25821	0.19593	0.43977	3.07349	3.31839	1.48953	3.14209
		0.874	0.925	0.977	0.683	0.997	0.984	0.976	0.991	0.990	0.998	0.892	0.997
	1.7	0.23378	0.31952	0.51540	0.39253	0.15942	0.27986	0.19097	0.40078	3.22159	3.46792	1.42785	2.74779
		0.988	0.990	0.978	0.808	0.929	0.880	0.928	0.931	0.987	0.995	0.897	0.699

Table 6: MSEs and ABs of the Bayes for the parameters p, α, λ_1 and λ_2 under Prior-I.

$(p, \alpha, \lambda_1, \lambda_2)$	n	T	$\tilde{p}$	$\tilde{\alpha}$	$\tilde{\lambda_1}$	$\tilde{\lambda_2}$
(0.5,0.5,0.5,0.6)	35	1	0.01303	0.02778	0.11147	0.05335
			-0.01916	-0.1771	0.26125	0.14728
		1.25	0.01274	0.02027	0.10858	0.05267
			-0.01778	-0.10731	0.24754	0.13591
		1.5	0.01105	0.01826	0.09907	0.05041
			-0.01701	-0.06724	0.23706	0.13169
	50	1	0.01028	0.02575	0.07483	0.03354
			-0.01683	-0.14925	0.23516	0.12452
		1.25	0.00924	0.01879	0.07113	0.03256
			-0.01612	-0.09424	0.22193	0.11926
		1.5	0.00828	0.01267	0.06692	0.03147
			-0.01443	-0.05613	0.21626	0.10957
	70	1	0.00689	0.02104	0.05569	0.02762
			-0.01579	-0.13957	0.22142	0.12043
		1.25	0.00668	0.01674	0.05552	0.02492
			-0.01590	-0.08218	0.20535	0.10444
		1.5	0.00547	0.01082	0.05343	0.02344
			-0.00992	-0.03981	0.19986	0.09937
(0.65,0.5,0.6,0.4)	35	1	0.02879	0.02625	0.05696	0.15935
			0.02427	-0.13006	0.16829	0.16359
		1.5	0.01895	0.01888	0.04445	0.13350
			0.01991	-0.08343	0.13305	0.13979
		1.7	0.01009	0.01747	0.03921	0.12484
			0.00896	-0.00719	0.12066	0.11820
	50	1	0.00937	0.02663	0.03493	0.12743
			0.01881	-0.11362	0.13648	0.19403
		1.5	0.00724	0.01426	0.02923	0.11502
			0.01551	-0.06278	0.11809	0.13433
		1.7	0.00697	0.01116	0.02304	0.10024
			0.00878	-0.05900	0.09500	0.11597
	70	1	0.00716	0.02203	0.02954	0.11698
			0.01139	-0.07286	0.13469	0.11506
		1.5	0.00515	0.01057	0.02513	0.11046
			0.01450	-0.05933	0.10898	0.11391
		1.7	0.00447	0.00885	0.02459	0.10635
			0.00801	-0.03410	0.10561	0.08584

Table 7: The HPD credible interival and coverage percentage(CP) of the Bayes for the parameters p, α, λ_1 and λ_2 under Prior-I.

$(p, \alpha, \lambda_1, \lambda_2)$	n	T	$\tilde{p}$	$\tilde{\alpha}$	$\tilde{\lambda_1}$	$\tilde{\lambda_2}$
(0.5,0.5,0.5,0.6)	35	1	0.27514	0.27742	0.72005	0.67363
			1.000	0.995	0.962	0.998
		1.25	0.23523	0.29105	0.62533	0.57796
			0.999	0.957	0.992	0.929
		1.5	0.21244	0.30519	0.57164	0.52712
			0.987	0.995	0.999	0.964
	50	1	0.21694	0.21071	0.57203	0.54804
			0.999	0.998	0.997	0.998
		1.25	0.18937	0.23257	0.51340	0.48732
			0.997	0.995	0.993	0.989
		1.5	0.16804	0.23775	0.46906	0.44318
			1.000	0.993	0.995	0.987
	70	1	0.16777	0.15925	0.46425	0.45078
			0.999	0.993	0.974	0.929
		1.25	0.14662	0.17371	0.41626	0.40160
			1.000	0.991	0.964	1.000
		1.5	0.13184	0.18608	0.37903	0.36581
			0.969	0.938	0.916	0.993
(0.65,0.5,0.6,0.4)	35	1	0.28298	0.25769	0.60367	0.58709
			1.000	0.962	1.000	1.000
		1.5	0.21315	0.30550	0.49406	0.48252
			0.999	0.991	0.993	0.998
		1.7	0.20444	0.31294	0.46805	0.45985
			0.997	0.994	0.989	0.993
	50	1	0.21967	0.19703	0.48438	0.47641
			0.999	0.976	1.000	0.989
		1.5	0.16415	0.23115	0.40269	0.39771
			1.000	0.997	1.000	0.999
		1.7	0.15387	0.24329	0.38041	0.37819
			1.000	0.961	0.995	0.997
	70	1	0.17191	0.14660	0.39378	0.38990
			0.998	0.987	0.991	0.996
		1.5	0.12441	0.18286	0.32689	0.32417
			0.936	0.978	1.000	0.999
		1.7	0.11601	0.18345	0.29832	0.29758
			0.998	0.998	0.984	0.997

Table 8: MSEs and ABs of the Bayes for the parameters p, α, λ_1 and λ_2 under Prior-II.

$(p, \alpha, \lambda_1, \lambda_2)$	n	T	$\tilde{p}$	$\tilde{\alpha}$	$\tilde{\lambda_1}$	$\tilde{\lambda_2}$
(0.5,0.5,0.5,0.6)	35	1	0.01341	0.03271	0.07689	0.04428
			-0.01760	-0.15917	0.19381	0.09275
		1.25	0.01165	0.02859	0.07210	0.03738
			-0.01625	-0.11833	0.17413	0.07831
		1.5	0.01136	0.01958	0.07083	0.03534
			-0.01156	-0.07891	0.15470	0.05505
	50	1	0.00988	0.03207	0.05324	0.02365
			-0.01638	-0.15546	0.18361	0.08153
		1.25	0.00964	0.02061	0.04794	0.02293
			-0.01268	-0.10969	0.17285	0.06749
		1.5	0.00839	0.01534	0.04591	0.02110
			-0.01166	-0.07661	0.15190	0.05219
	70	1	0.00741	0.02919	0.05134	0.02113
			-0.01312	-0.06791	0.18302	0.07319
		1.25	0.00718	0.01964	0.04359	0.01783
			-0.01107	-0.06031	0.14945	0.06194
		1.5	0.00602	0.01290	0.03828	0.01260
			-0.00943	-0.01699	0.13797	0.03726
(0.65,0.5,0.6,0.4)	35	1	0.03742	0.02709	0.05693	0.15959
			0.03426	-0.12681	0.16754	0.11772
		1.5	0.01353	0.02059	0.05024	0.14618
			0.01331	-0.03491	0.15088	0.11730
		1.7	0.00923	0.01907	0.04058	0.12591
			0.00868	-0.02682	0.11947	0.06425
	50	1	0.00905	0.02608	0.03292	0.13054
			0.02230	-0.13760	0.13103	0.10783
		1.5	0.00702	0.01341	0.03059	0.12262
			0.01103	-0.05579	0.11983	0.10613
		1.7	0.00647	0.01262	0.02848	0.10916
			0.00707	-0.03064	0.10438	0.10309
	70	1	0.00720	0.02022	0.02844	0.11636
			0.02674	-0.15040	0.13072	0.12098
		1.5	0.00523	0.01012	0.02497	0.10351
			0.01331	-0.05568	0.11924	0.08602
		1.7	0.00469	0.00852	0.01948	0.09368
			0.00480	0.00097	0.08651	0.04700

Table 9: The HPD credible interival and coverage percentage(CP) of the Bayes for the parameters p, α, λ_1 and λ_2 under Prior-II.

$(p, \alpha, \lambda_1, \lambda_2)$	n	T	$\tilde{p}$	$\tilde{\alpha}$	$\tilde{\lambda_1}$	$\tilde{\lambda_2}$
(0.5,0.5,0.5,0.6)	35	1	0.26495	0.26073	0.69141	0.63604
			1.000	0.949	0.955	0.998
		1.25	0.23626	0.27733	0.62074	0.56481
			0.999	1.000	0.976	0.989
		1.5	0.20837	0.29537	0.56546	0.51615
			1.000	0.998	0.995	0.999
	50	1	0.21223	0.20343	0.56386	0.53499
			0.984	0.990	0.995	0.997
		1.25	0.19156	0.21965	0.50283	0.47203
			0.989	0.992	0.978	0.951
		1.5	0.16778	0.23107	0.46161	0.43485
			1.000	0.969	0.998	0.940
	70	1	0.16689	0.15960	0.45412	0.43868
			0.993	0.877	0.994	0.999
		1.25	0.14662	0.17337	0.41144	0.39504
			0.998	0.963	0.944	0.988
		1.5	0.13103	0.18351	0.37451	0.35942
			0.998	0.976	0.934	0.978
(0.65,0.5,0.6,0.4)	35	1	0.284104	0.26480	0.60504	0.59145
			1.000	1.000	1.000	1.000
		1.5	0.21155	0.31846	0.49620	0.48523
			0.996	0.991	0.991	0.997
		1.7	0.19823	0.32933	0.47330	0.46822
			0.997	1.000	0.989	0.998
	50	1	0.21957	0.19975	0.48523	0.47788
			0.993	0.997	0.996	0.966
		1.5	0.16405	0.23582	0.39915	0.39335
			0.997	0.953	0.989	0.997
		1.7	0.15270	0.24349	0.37822	0.37619
			1.000	0.991	0.997	0.998
	70	1	0.17099	0.15024	0.39304	0.38904
			0.919	0.993	0.978	0.893
		1.5	0.12573	0.18266	0.32549	0.32331
			0.995	0.999	0.991	0.949
		1.7	0.11474	0.18385	0.29796	0.29787
			0.999	0.997	0.992	0.985

8.1 Carbon fiber data

Here, we apply a real data set which was originally reported by Bader and Priest (1982). The data represents the strength measured in GPA for single carbon fibres and impregnated 1000-carbon fibre tows. Single fibres were tested under tension at gauge lengths of 20 mm with sample sizes $n = 69$. The data divided by 10 for computational convenience are as follows:

0.1312, 0.1314, 0.1479, 0.1552, 0.1700, 0.1803, 0.1861, 0.1865, 0.1944, 0.1958, 0.1966, 0.1997, 0.2006, 0.2021, 0.2027, 0.2055, 0.2063, 0.2098, 0.2140, 0.2179, 0.2224, 0.2240, 0.2253, 0.2270, 0.2272, 0.2274, 0.2301, 0.2301, 0.2359, 0.2382, 0.2382, 0.2426, 0.2434, 0.2435, 0.2478, 0.2490, 0.2511, 0.2514, 0.2535, 0.2554, 0.2566, 0.2570, 0.2586, 0.2629, 0.2633, 0.2642, 0.2648, 0.2684, 0.2697, 0.2726, 0.2770, 0.2773, 0.2800, 0.2809, 0.2818, 0.2821, 0.2848, 0.2880, 0.2954, 0.3012, 0.3067, 0.3084, 0.3090, 0.3096, 0.3128, 0.3233, 0.3433, 0.3585, 0.3585.

In order to perform the classical and Bayesian analysis assuming the two-component mixture of GR distribution, we randomly assembled the sets of data into two subpopulations using probabilistic mixing weight $p_1 = 0.45$ and $T = 3.08$. We call the first set of data as Data-I with the subpopulations as follows:

Subpopulation-I:

0.1312, 0.1479, 0.1552, 0.1700, 0.1861, 0.1944, 0.1997, 0.2027, 0.2063, 0.2179, 0.2240, 0.2270, 0.2301, 0.2382, 0.2426, 0.2434, 0.2478, 0.2514, 0.2570, 0.2633, 0.2684, 0.2770, 0.2773, 0.2800, 0.2818, 0.2821, 0.2880, 0.3012, 0.3067, 0.3233, 0.3585.

Subpopulation-II:

0.1314, 0.1803, 0.1865, 0.1958, 0.1966, 0.2006, 0.2021, 0.2055, 0.2098, 0.2140, 0.2224, 0.2253, 0.2272, 0.2274, 0.2359, 0.2435, 0.2490, 0.2511, 0.2535, 0.2554, 0.2566, 0.2586, 0.2629, 0.2642, 0.2648, 0.2697, 0.2726, 0.2809, 0.2848, 0.2954, 0.3084, 0.3090, 0.3096, 0.3128, 0.3433, 0.3128, 0.3433, 0.3585.

We call the second set of data as Data-II with subpopulations of the given carbon fiber data set as follows:

Subpopulation-I:

0.1312, 0.1314, 0.1700, 0.1861, 0.1944, 0.1997, 0.2006, 0.2021, 0.2098, 0.2240, 0.2270, 0.2274, 0.2301, 0.2359, 0.2382, 0.2426, 0.2490, 0.2566, 0.2629, 0.2642, 0.2697, 0.2726, 0.2770, 0.2800, 0.2821, 0.3012, 0.3084, 0.3090, 0.3233, 0.3585, 0.3585.

Subpopulation-II:

0.1479, 0.1552, 0.1803, 0.1865, 0.1958, 0.1966, 0.2027, 0.2055, 0.2063, 0.2140, 0.2179, 0.2224, 0.2253, 0.2272, 0.2434 , 0.2435, 0.2478, 0.2511, 0.2514, 0.2535, 0.2554, 0.2570, 0.2586, 0.2633, 0.2648, 0.2684 ,0.2773, 0.2809, 0.2818, 0.2848, 0.2880, 0.2954, 0.3067, 0.3096, 0.3128 ,0.3433 .

Now, before we obtain the various point and interval estimates to see the performance of the different methodologies discussed, it is essential to check whether the given data set fits our model. For this purpose, we calculate Kolmogorov-Smirnov(KS) distance and p-values. For comparison, together with MTGR distribution, we consider some other models namely, generalized Rayleigh distribution(GR), generalized exponential distribution (GE), and exponentiated Pareto distribution (EP) and calculate the associated KS distance and p-values along with MLEs of the parameters. We have calculated $MTGR_1$ and $MTGR_2$ based on the estimates under Data-I and Data-II, respectively. All the calculated values are tabulated in Table 10. From the tabulated values, one may easily conclude that the MTGR model shows a reasonably better fit than the other competing models for the considered data. Furthermore, plots for the empirical cumulative distribution function with the theoretical cumulative distribution function of the distribution are also provided in Figure 11, which also suggest a comparably better fit of the considered MTGR distribution.

Table 10: MLEs of parameters and goodness fit test for the real data.

Model	MLE	KS-distance	p-value	Standard error
$MTGR_1$	$\hat{p}$=0.4412, $\hat{\alpha}$=8.8870, $\hat{\lambda}_1$=6.9047,$\hat{\lambda}_2$=6.4676	0.06178	0.9549	0.00646
$MTGR_2$	$\hat{p}$=0.4627, $\hat{\alpha}$=9.4985, $\hat{\lambda}_1$=6.7616,$\hat{\lambda}_2$=6.7536	0.06268	0.9492	0.00623
EP	$\hat{\alpha} = 134.0172$, $\hat{\lambda} = 24.7305$	0.10185	0.4713	0.00803
GE	$\hat{\alpha} = 88.2219$, $\hat{\lambda} = 20.3746$	0.09496	0.5625	0.00755
GR	$\hat{\alpha}$=8.7898, $\hat{\lambda}$=6.6674	0.06586	0.9257	0.00638

Table 11: Point and interval estimates of p, α, λ_1 and λ_2 for data-I.

Carbon fiber data	$\tilde{p}$	$\tilde{\alpha}$	$\tilde{\lambda_1}$	$\tilde{\lambda_2}$
MLE	0.44914	0.44751	1.41013	1.37833
ACL	[0.21583]	[0.27301]	[0.24792]	[0.88127]
Boot-p	[0.17391]	[0.15662]	[0.18653]	[0.27889]
Boot-t	[2.93456]	[3.38393]	[1.77952]	[1.70521]
Bayes(Prior-I)	0.46427	0.43892	1.45865	1.50586
HPD length	[0.09825]	[0.08713]	[0.12376]	[0.24327]
Bayes(Prior-II)	0.46476	0.58590	1.52089	1.56184
HPD length	[0.10985]	[0.12665]	[0.08086]	[0.17406]

In Tables 11 and 12, we report MLEs, 95% approximate CIs, Bayes point estimates based on Prior-I and Prior-II, 95% HPD credible intervals. In addition to these, we also report boot-p and boot-t intervals for each parameter of the MTGR distribution. From Tables 11 and 12, we observe that Bayesian point estimates perform quite good than the ML estimates for Data-I and Data-II both under both the prior assumptions. Here we have considered not informative priors. When comparing the various classical interval estimates namely approximate, boot-p and boot-t intervals with the HPD interval estimates under the two priors, we observe that the performance of the HPD intervals is better in terms of interval lengths. Further comparing the point and interval estimates under classical and Bayesian approaches for the two data sets, we observe that the results for Data-II perform better. One may also make some other observations based on

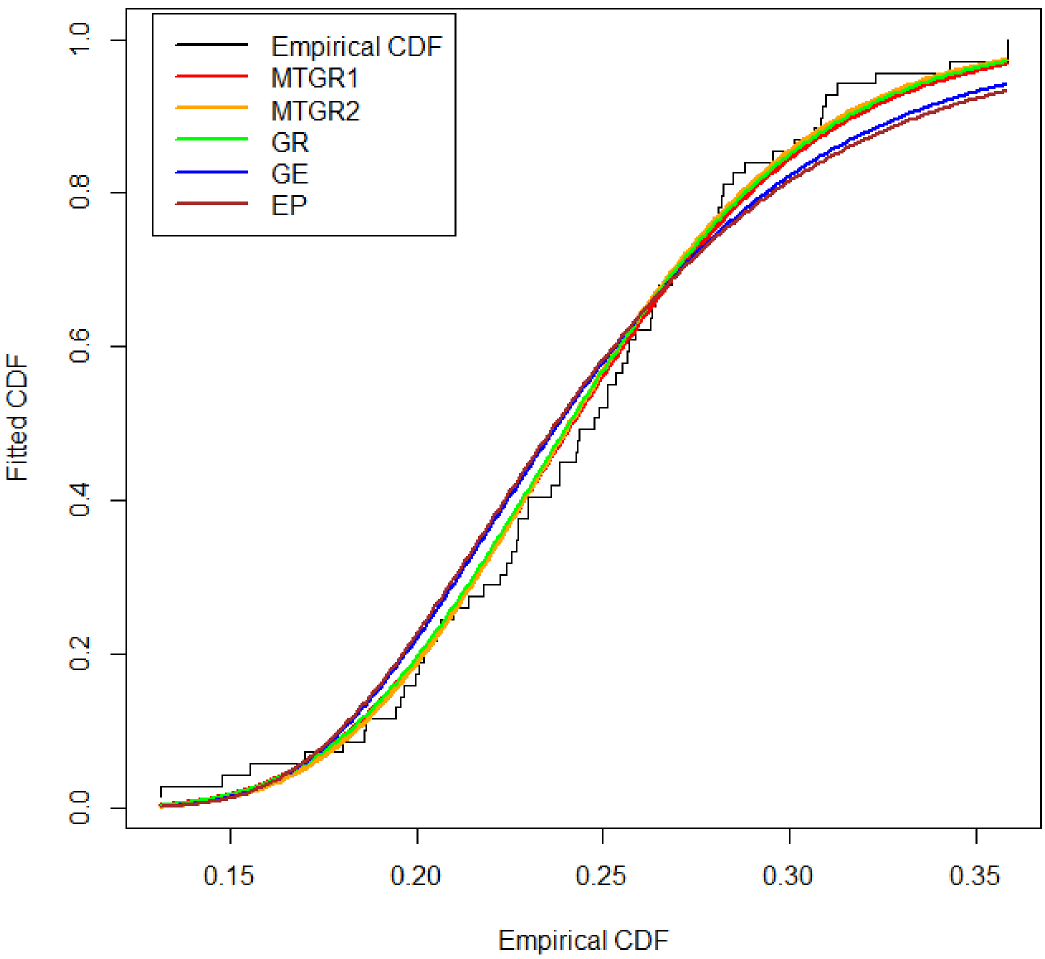

Figure 11: Empirical and fitted CDFs for the different distributions.

Table 12: Point and interval estimates of p, α, λ_1 and λ_2 for data-II.

Carbon fiber data	$\tilde{p}$	$\tilde{\alpha}$	$\tilde{\lambda_1}$	$\tilde{\lambda_2}$
MLE	0.46268	0.44500	1.39485	1.39631
ACL	[0.03577]	[0.29634]	[0.24792]	[1.30890]
Boot-p	[0.17911]	[0.15277]	[0.18928]	[0.37945]
Boot-t	[2.95780]	[3.4009]	[1.81881]	[1.797794]
Bayes (Prior-I)	0.46474	0.43493	1.43119	1.59457
HPD length	[0.00099]	[0.07051]	[0.07162]	[0.33376]
Bayes(Prior-II)	0.46215	0.50196	1.49257	1.69332
HPD length	[0.00087]	[0.09827]	[0.04581]	[0.28211]

estimates of parameters and other comparisons may also be made. Here we have considered the two data sets based on probabilistic mixing weight $p = 0.45$ and $T = 3.08$, by changing the values of these two quantities, further interesting observations can also be drawn.

8.2 Floyd River floods data

The occurrence of extreme flood rates in rivers has significant implications for the economy, society, politics, and engineering. A prime example of this is the 1993 floods along the Mississippi River. Therefore, it is crucial to model flood data and conduct analyses that involve predicting extreme values such as the maximum flood levels expected once every fifty or thousand years. These applications of extreme value theory play a vital role. This data was originally taken by Mudholkar et al. (1995) and presented in Table 13. Although there are various distribution models used in this context, Pericchi and Rodriguez-Iturbe (1985) argue that the Gumbel distribution, which represents a medium-tail extreme-value distribution, is the only one with a theoretical basis suitable for analyzing extreme streamflow. The following data shows the consecutive annual flood discharge rates for the Floyd River at James, Iowa, for the years 1955-1973. For the

Table 13: The consecutive annual Floyd River flood discharge rate data at James, Iowa.

Year	Flood discharge in (ft^3/s)
1955-1964	2260,318,1330,970,1920,15100,2870,20600,3810,726
1965-1973	7500,7170,2000,829,17300,4740,13400,2940,5660.

Source: United State Water Resources Council (1977).

goodnessfit of this data, we first divide by 10000 and calculate Kolmogorov-Smirnov(KS) distance and p-values and present the values along with MLE in Table 14. From the tabulated values, one may easily conclude that the MTGR model shows a reasonably better fit than the other competing models for the considered data. Furthermore, plots for the empirical cumulative distribution function with the theoretical cumulative distribution function of the distribution are also provided in Figure 12 which also suggest a comparably better fit of the considered MTGR distribution. In Table 15, we report

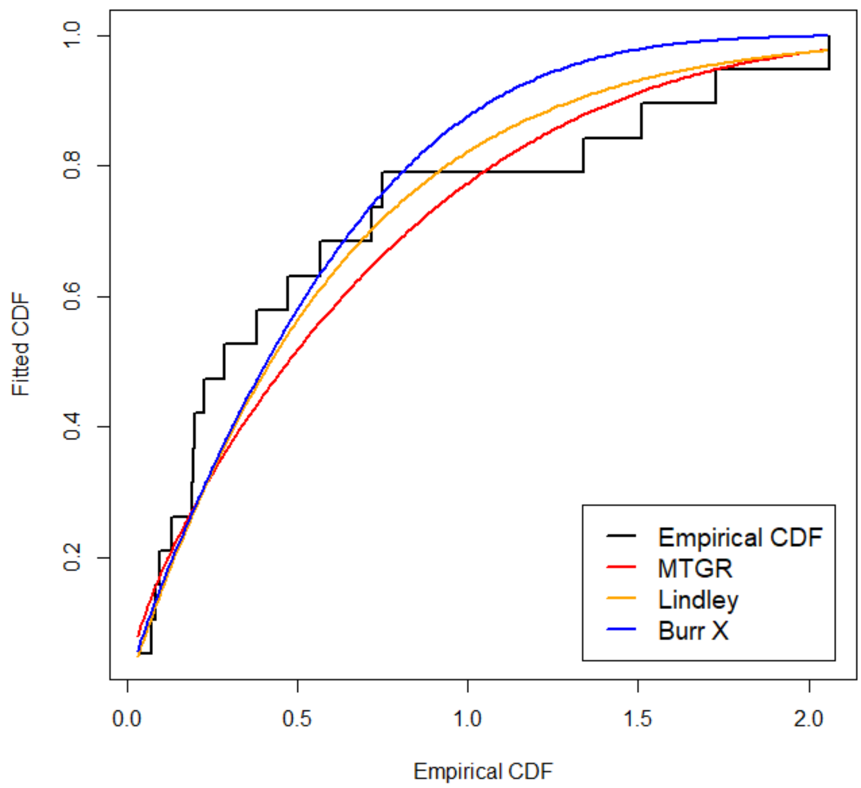

Figure 12: Empirical and fitted CDFs for the different distributions under Floyd River flood data.

MLEs, 95% approximate CIs, Bayes point estimates based on Prior-I and Prior-II, 95% HPD credible intervals. In addition to these, we also report boot-p and boot-t intervals for each parameter of the MTGR distribution. From Table 15, we observe that Bayesian estimates perform quite good than the ML estimates for river flood data under non-informative prior.

9 Conclusion

In this article, we have considered the classical and Bayesian methods of estimation of MTGR distribution using type I censored samples. In addition, we have derived some statistical properties along with the identifiability of MTGR distribution. From simulation and real-life data analysis, we may conclude that the Bayesian estimation

Table 14: MLEs of parameters and goodness fit test for the Floyd River flood data.

Model	MLE	KS-distance	p-value	Standard error
MTGR	$\hat{p}$=0.5263, $\hat{\alpha}$=0.3456, $\hat{\lambda}_1$=0.8025,$\hat{\lambda}_2$=0.8046	0.16794	0.5992	0.1291
Lindley	$\hat{\alpha}$=2.3240	0.1877	0.4596	0.1213
Burr X	$\hat{\alpha}$=0.3202, $\hat{\beta}$=0.7870	0.1907	0.4398	0.13096

Table 15: Point and interval estimates of $p,\ \alpha,\ \lambda_1$ and λ_2 for Floyd river flood data.

	$\tilde{p}$	$\tilde{\alpha}$	$\tilde{\lambda_1}$	$\tilde{\lambda_2}$
MLE	0.50605	0.48077	1.28281	0.87915
ACL	[0.43929]	[0.60831]	[1.66668]	[0.93242]
Boot-p	[0.36529]	[0.35900]	[0.64301]	[0.44014]
Boot-t	[3.30656]	[3.29592]	[2.52984]	[1.76961]
Bayes (Prior-I)	0.54984	0.40896	1.09845	0.81905
HPD length	[0.23180]	[0.17481]	[0.78118]	[0.54513]
Bayes(Prior-II)	0.5135	0.5195	1.17413	0.9598
HPD length	[0.12874]	[0.29780]	[0.67476]	[0.44562]

has an edge over ML method. An application of the MTGR distribution to real data set shows the feasibility of our proposed distribution. We hope the proposed MTGR distribution may attract wider application in statistics. In future, this work can be extended using more than 2-component mixture of GR distribution using informative and non-informative priors. Moreover, numerical methods such as EM algorithm and Laplace methods are worth to be studied. Additionally, a finite mixture of regression models for complete and censored data based on MTGR distributions can be considered. More importantly, burn-in procedures that are used engineering methods to eliminate weak components through determining optimal stopping time are worth to be studied using the current distribution. This can also be achieved by studying the relation between the change points of mean residual life and failure rate. Finally, further information pertaining to the proportion of the weak components which will fail should be carried out, which can be quantified by estimating the entropy parameter of the MTGR distribution. It is worth mentioning that the entropy parameter can be estimated using some methods given in Shakhatreh et al. (2021).

Acknowledgement

We thank the Associate Editor and anonymous reviewers for their constructive comments and suggestions that greatly improved this paper.

References

Abramowitz, M.and Stegun, I. (1965). *Handbook of Mathematical Functions*. New York.

Acheson, M. and McElwee, E. (1953). Concerning the reliability of electron tubes. In *Proceedings of the IREs*, volume 40, pages 1204 – 1206.

Ahmad, K. (1988). Identifiability of finite mixtures using a new transform. *Annals of the Institute of Statistical Mathematics*, 40:261–265.

Ahmad, K. and Abd-El-Hakim, N. (1990). The identifiability of finite mixing of some noncentral distributions. *Applied Mathematics Letters*, 3:1–3.

Al-Hemyari, Z. A. and Al Abbasi, J. N. (2023). Modelling and analysing the daily temperature of several cities using mixture gaussian distributions. *International Journal of Computing Science and Mathematics*.

Al-Hussaini, E. and Ahmad, K. (1981). On the identifiability of finite mixture of distributions. *IEEE Transactions on Information Theory*, 27:664–668.

Al-Hussaini, E. and Sultan, K. (2001). Reliability and hazard based on finite mixture models. Balakrishnan, N., Rao, C.R. (eds.). *Handbook of Statistics*, 20:139–183.

Ali, S. (2014). Mixture of the inverse Rayleigh distribution: Properties and estimation in Bayesian framework. *Applied Mathematical Modelling*, 39:515–530.

Ali, S., Aslam, M., Kundu, D., and Kazmi, S. M. A. (2012). Bayesian estimation of the mixture of generalized exponential distribution: a versatile lifetime model in industrial processes. *Journal of the Chinese Institute of Industrial Engineers*, 29(4):246–269.

Alotaibi, R., Nassar, M., Ghosh, I., Rezk, H., and Elshahhat, A. (2022). Inferences of a mixture bivariate alpha power exponential model with engineering application. *Axioms*, 9(11):459.

Aslam, M., Ali, S., Yousaf, R., and Shah, I. (2020). Mixture of transmuted Pareto distribution: Properties, applications and estimation under Bayesian framework. *Journal of the Franklin Institute*, 357:2934–2957.

Aslam, M., Nawaz, Ali, S., and Silva, S. (2018). Bayesian estimation of the mixture of exponentiated inverted weibull distribution using noninformative and informative priors. *Journal of the National Science Foundation of Sri Lanka*, 46:569—586.

Aslam1, M., Tahir, M., Hussain, Z., and Al-Zahrani, B. (2015). A 3-component mixture of Rayleigh distributions: Properties and estimation in bayesian framework. *PLoS ONE*, 10.

Atienza, N., Garcia-Heras, J., and Muñoz Pichardo, J. (2006). A new condition for identifiability of finite mixture distributions. *Metrika*, 63:215—221.

Bader, M. G. and Priest, A. M. (1982). Statistical aspects of fibre and bundle strength in hybrid composites. *Progress in science and engineering of composites*, pages 1129–1136.

Bdair, O. M. and Raqab, M. Z. (2022). Prediction of future censored lifetimes from mixture exponential distribution. *Metrika*, pages 1–25.

Bhattacharya, C. G. (1967). A simple method of resolution of a distribution into gaussian components. *Biometrics*, 23:115–135.

Burckhardt, C. B. (1978). Speckle in ultrasound B-mode scans. *IEEE Transactions on Sonics and ultrasonics*, 25:1–6.

Chandra, S. (1977). On the mixtures of probability distributions. *Scand. J. Stat.*, 4:105–112.

Chen, M. H. and Shao, Q. M. (1999). Monte carlo estimation of bayesian credible and hpd intervals. *Journal of Computational and Graphical Statistics*, 8:69–92.

Chivers, R. C. (1977). The scattering of ultrasound by human tissues—some theoretical models. *Ultrasound in medicine and biology*, 3:1–13.

Choudhury, A. (2005). A simple derivation of moments of the exponentiated weibull distribution. *Metrika*, 62:17—22.

Dey, S., Dey, T., and Luckett, D. (2017). Statistical inference for the generalized rayleigh distribution based on upper record values. *Model Assisted Statistics and Applications*, 12:15–29.

Efron, B. and Tibshirani, R. (1994). *An introduction to the bootstrap.* Chapman and Hall, New York, NY.

Feroze, N. and Aslam, M. (2014). Bayesian analysis of doubly censored lifetime data using two component mixture of weibull distribution. *Journal of the National Science Foundation of Sri Lanka*, 42:325—334.

Feroze, N., Aslam, M., Sindhu, T. N., and Noor-ul Amin, M. (2021). Mixed weibull distributions for the bayesian analysis of reliability when failures are progressively censored. *Journal of Statistical Computation and Simulation*, 91:3505–3529.

Gregor, J. (1969). An algorithm for the decomposition of a distribution into gaussian components. *Biometrics*, 25:79–93.

Harris, C. M. (1983). On finite mixtures of geometric and negative binomial distributions. *Communications in Statistics-Theory and Methods*, 12:987–1007.

Hastings, W. K. (1970). Monte carlo sampling methods using markov chains and their applications. *Biometrika*, 57:97–109.

Jahanbani, E., Najafabadi, A. T. P., and Masoumifard, K. (2023). On bayesian credibility mean for finite mixture distributions. *Annals of Actuarial Science*, pages 1–25.

Jedidi, K., Jagpal, H. S., and DeSarbo, W. S. (1997). Finite-mixture structural equation models for response-based segmentation and unobserved heterogeneity. *Marketing Science*, 16:39–59.

Junru, R. E. N. and Wenhao, G. U. I. (2020). A statistical inference for generalized Rayleigh model under type-ii progressive censoring with binomial removals. *Journal of Systems Engineering and Electronics*, 31:206–223.

Kalantan, Z. and F., A. (1988). A 2-component laplace mixture model: Properties and parametric estimations. *Mathematics and Statistics*, 7:9–16.

Kundu, D. and Raqab, M. Z. (2005). Generalized Rayleigh distribution: different methods of estimations. *Computational statistics and data analysis*, 49:187–200.

Li, L. and Sedransk, N. (1988). Mixtures of distributions: A topological approach. *The Annals of Statistics,*, 16:1623—1634.

Li, Y. and Fang, K. T. (2022). A new approach to parameter estimation of mixture of two normal distributions. *Communications in Statistics-Simulation and Computation*, pages 1–27.

Mahto, A. K., Tripathi, Y. M., and Dey, S. (2018). Estimation of density and distribution functions of a burr X distribution. *Journal of Statistical Research*, 52:43–59.

Mendenhall, W. and Hader, R. (1958). Estimation of parameters of mixed exponentially distributed failure time distributions from censored life test data. *Biometrika*, 45(3-4):504–520.

Metropolis, N., Rosenbluth, A. W., Rosenbluth, M. N., Teller, A. H., and Teller, E. (1953). Equation of state calculations by fast computing machines. *The journal of chemical physics*, 21:1087–1092.

Mudholkar, G., Srivastava, D., and Freimer, G. (1995). The exponentiated Weibull family: a reanalysis of the bus-motor-failure. *Technometrics*, 37:436–445.

Nadarajah, S. and Kotz, S. (2005). Information matrix for a mixture of two pareto distributions. *Iranian Journal of Science and Technology, Transaction A*, 29:379–385.

Newcomb, S. (1886). A generalized theory of the combination of observations so as to obtain the best result. *American Journal of Mathematics*, 8:343—366.

Otiniano, C., Rathie, P., and Ozelimc, L. (2015). On the identifiability of finite mixture of skew-normal and skew-t distributions. *Statistics and Probability Letters*, 106:103—-108.

Otiniano, C. E. G., Gonçalves, C. R., and Dorea, C. C. Y. (2017). Mixture of extreme-value distributions: identifiability and estimation. *Communications in Statistics – Theory and Methods*, 46:6528–6542.

Saleem, M., Aslam, M., and Economus, P. (2010). On the bayesian analysis of the mixture of power distribution using the complete and censored sample. *Journal of Applied Statistics*, 37:25–40.

Sankaran, P. and Nair, M. (2005). On a finite mixture of pareto distributions. *Calcutta Statistical Association Bulletin*, 57:225–226.

Shakhatreh, M. K., Dey, S., and Alodat, M. (2021). Objective bayesian analysis for the differential entropy of the weibull distribution. *Applied Mathematical modelling*, 89:314–332.

Shakhatreh, M. K., Lemonte, A. J., and Moreno-–Arenas, G. (2019). The log-normal modified weibull distribution and its reliability implications. *Reliability Engineering and System Safety*, 188:6–22.

Shawky, A. I. and Bakoban, R. A. (2009). On finite mixture of two-component exponentiated gamma distribution. *Journal of Applied Sciences Research*, 5:1351–1369.

Sindhu, T. N., Khan, H., Zawar Hussain, Z., and Al-Zahrani, B. (2018). Bayesian inference from the mixture of half-normal distributions under censoring. *Journal of the National Science Foundation of Sri Lanka*, 46:587—600.

Sultan, K. S., Ismail, M. A., and Al-Moisheer, A. S. (2007). Mixture of two inverse weibull distributions: Properties and estimation. *Computational Statistics and Data Analysis*, 51:5377–5387.

Surles, J. and Padgett, W. (2001). Inference for reliability and stress-strength for a scaled Burr type X distribution. *Lifetime Data Analysis*, 7:187–200.

Tahir, M., Aslam, M., Hussain, Z., Abid1, M., Sajid, A., and Ahsanullah, M. (2019). A 3–component mixture of exponential distribution assuming doubly censored data: Properties and bayesian estimation. *Journal of Statistical Theory and Applications*, 19:197–21.

Tahir, M., Aslam, M., Hussain, Z., and Khan, A. (2016). On finite 3-component mixture of exponential distributions: Properties and estimation. *Cogent Mathematics*, 3:1–23.

Teicher, H. (1963). Identifiability of finite mixtures. *Annals of the Institute of Statistical Mathematics*, 34:1265—1269.

Yakubu, A. and Yahaya, A. (2015). Bayesian estimation for the shape parameter of generalized rayleig1h distribution under non-informative prior. *International Journal of Advanced Statistics and Probability*, 4(1):1–10.

Appendix:

Elements of the observed information matrix for the MTGR model are given below.

$$\frac{\partial^2 \log L}{\partial p^2} = -\frac{r_1}{p^2} - \frac{r_2}{(1-p)^2} - \frac{(n-r)(F_1(T)-F_2(T))^2}{(1-F(T))^2},$$

$$\begin{aligned}\frac{\partial^2 \log L}{\partial p\,\partial \alpha} = & \frac{-(n-r)(F_1(T)-F_2(T))}{(1-F(T))^2}\{pF_1(T)\ln A_1(T) + (1-p)F_2(T)\ln A_2(T)\} \\ & - \frac{(n-r)}{1-F(T)}\{F_1(T)\ln A_1(T) - F_2(T)\ln A_2(T)\},\end{aligned}$$

$$\frac{\partial^2 \log L}{\partial p\,\partial \lambda_1} = -\frac{(n-r)T}{\lambda_1(1-F(T))}f_1(T) - \frac{p(n-r)T}{\lambda_1(1-F(T))^2}(F_1(T)-F_2(T))f_1(T),$$

$$\frac{\partial^2 \log L}{\partial p\,\partial \lambda_2} = \frac{(n-r)T}{\lambda_2(1-F(T))}f_2(T) + \frac{p(n-r)T}{\lambda_2(1-F(T))^2}(F_1(T)-F_2(T))f_2(T),$$

$$\begin{aligned}\frac{\partial^2 \log L}{\partial \lambda_1^2} = & -\frac{2r_1}{\lambda_1^2} - 2\sum_{j=1}^{r_1} x_{1j}^2 + 2(\alpha-1)\sum_{j=1}^{r_1}\frac{x_{1j}^2 e^{-\lambda_1^2 x_{1j}^2}}{A_1(x_{2j})} \\ & - 4(\alpha-1)\sum_{j=1}^{r_1}\left\{\lambda_1 x_{1j}^2\frac{B_1(x_{1j})}{A_1(x_{1j})} + \frac{B_1^2(x_{1j})}{A_1^2(x_{1j})}\right\} \\ & - \frac{p(n-r)}{\lambda_1(1-F(T))}\left\{\frac{2}{\lambda_1}f_1(T) - 2\lambda_1 T^2 f_1(T) \right. \\ & \left. + \frac{2(\alpha-1)B_1(T)}{A_1(T)}f_1(T)\right\} \\ & + \frac{p(n-r)T}{\lambda_1^2(1-F(T))^2}\{1-F(T)-pTf_1(T)\}f_1(T),\end{aligned}$$

$$\frac{\partial^2 \log L}{\partial\lambda_1\,\partial\lambda_2} = -\frac{p(1-p)(n-r)T^2}{\lambda_1\lambda_2(1-F(T))^2} f_1(T) f_2(T),$$

$$\begin{aligned}\frac{\partial^2 \log L}{\partial\lambda_1\partial\alpha} = {} & 2\lambda_1 \sum_{j=1}^{r_1} \frac{x_{1j}^2 e^{-\lambda_1^2 x_{1j}^2}}{A_1(x_{1j})} - \frac{p(n-r)T}{\lambda_1(1-F(T))^2}\Big\{pF_1(T)\ln F_1(T) \\ & + (1-p)F_2(T)\ln F_2(T)\Big\} f_1(T) \\ & - \frac{p(n-r)T}{\lambda_1(1-F(T))}(\alpha^{-1} + \ln A_1(T)) f_1(T),\end{aligned}$$

$$\begin{aligned}\frac{\partial^2 \log L}{\partial\lambda_2^2} = {} & -\frac{2r_2}{\lambda_2^2} - 2\sum_{j=1}^{r_2} x_{2j}^2 + 2(\alpha-1)\sum_{j=1}^{r_2} \frac{x_{2j}^2 e^{-\lambda_2^2 x_{2j}^2}}{A_2(x_{2j})} \\ & - 4(\alpha-1)\sum_{j=1}^{r_2}\Big\{\lambda_2 x_{2j}^2 \frac{B_2(x_{1j})}{A_2(x_{1j})} + \frac{B_2^2(x_{2j})}{A_2^2(x_{2j})}\Big\} \\ & - \frac{p(n-r)T}{\lambda_2(1-F(T))}\Big\{\frac{2}{\lambda_2} f_2(T) - 2\lambda_2 T^2 f_2(T) + \frac{2(\alpha-1)B_2(T)}{A_2(T)} f_2(T)\Big\} \\ & + \frac{p(n-r)T}{\lambda_2^2(1-F(T))^2}\{1 - F(T) - (1-p)T f_2(T)\} f_2(T),\end{aligned}$$

$$\begin{aligned}\frac{\partial^2 \log L}{\partial\lambda_2\,\partial\alpha} = {} & 2\lambda_2 \sum_{j=1}^{r_2} \frac{x_{2j}^2 e^{-\lambda_2^2 x_{2j}^2}}{A_2(x_{2j})} - \frac{p(n-r)T}{\lambda_2(1-F(T))^2}\Big\{pF_1(T)\ln F_1(T) \\ & + (1-p)F_2(T)\ln F_2(T)\Big\} f_2(T) \\ & - \frac{p(n-r)T}{\lambda_1(1-F(T))}(\alpha^{-1} + \ln A_2(T)) f_2(T),\end{aligned}$$

$$\begin{aligned}\frac{\partial^2 \log L}{\partial\alpha^2} = {} & -\frac{r}{\alpha^2} - \frac{(n-r)}{(1-F(T))^2}\big(pF_1(T)\ln A_1(T) + (1-p)F_2(T)\ln A_2(T)\big)^2 \\ & - \frac{(n-r)}{1-F(T)}\big(pF_1(T)(\ln A_1(T))^2 + (1-p)(\ln A_2(T))^2\big).\end{aligned}$$

where, $A_i(x) = 1 - e^{-\lambda_i^2 x^2}$ and $B_i(x) = \lambda_i x^2 e^{-\lambda_i^2 x^2},\ i = 1, 2.$